

Byzantines can also Learn from History: Fall of Centered Clipping in Federated Learning

Kerem Özfatura

KUIS AI Center

Koç University

aозfatura22@ku.edu.tr

Emre Özfatura

IPC Lab

Imperial College London

m.ozfatura@imperial.ac.uk

Alptekin Küpçü

Dept. of Computer Engineering

Koç University

akupcu@ku.edu.tr

Deniz Gunduz

IPC Lab

Imperial College London

d.gunduz@imperial.ac.uk

Abstract—The increasing popularity of the federated learning (FL) framework due to its success in a wide range of collaborative learning tasks also induces certain security concerns. Among many vulnerabilities, the risk of Byzantine attacks is of particular concern, which refers to the possibility of malicious clients participating in the learning process. Hence, a crucial objective in FL is to neutralize the potential impact of Byzantine attacks, and to ensure that the final model is trustable. It has been observed that the higher the variance among the clients’ models/updates, the more space there is for Byzantine attacks to be hidden. As a consequence, by utilizing momentum, and thus, reducing the variance, it is possible to weaken the strength of known Byzantine attacks. The *centered clipping* (CC) framework has further shown that, the momentum term from the previous iteration, besides reducing the variance, can be used as a reference point to neutralize Byzantine attacks better. In this work, we first expose vulnerabilities of CC framework, and introduce a novel attack strategy that can circumvent its defences and other robust aggregators by reducing test accuracy up to %33 on best-case scenarios in image classification tasks. Then, we propose a new robust and fast defence mechanism to prevent the proposed attack and other existing Byzantine attacks.

I. INTRODUCTION

Federated learning (FL) is a novel learning paradigm introduced as an alternative to centralized learning. The objective of FL [33] is to enable large-scale *collaborative learning* in a distributed manner, possibly at edge devices and without sharing local datasets, addressing, to some extent, the privacy concerns of the end-users. In FL, the learning process is often orchestrated by a central entity called the *parameter server* (PS). Participating clients first update their local models using their local private datasets, and then communicate their local models with the PS to seek a consensus with other participating clients. The PS utilizes an aggregation rule to obtain the consensus/global model based on the clients’ local models, and sends the consensus model back to the clients to repeat the process until the model achieves a certain generalization capability.

Since FL allows on-device training and can be scaled a large number of clients, it has become the *de facto* solution for several practical and commercialized implementations, e.g., learning keyboard prediction mechanisms on edge devices [20], [39], or digital healthcare /remote diagnosis [30], [32],

[40]. However, its widespread popularity also accompanies certain concerns regarding privacy, security, and robustness, particularly for those applications involving highly sensitive financial [29] or medical datasets [19], [23]. Hence, ultimately, the target is to make FL secure, privacy-preserving [10], [53], and robust against data heterogeneity [12].

With the scaling of FL, the PS has less control over the participating clients: that is, malicious clients can also participate in the learning process with the goal of impairing the final model. Thus, the key challenge for FL is to ensure that the consensus model is trustable despite the potential presence of *adversaries*. In the machine learning (ML) literature, adversaries have been studied in many different contexts and scenarios. In a broad sense, adversaries can be analyzed from the perspective of *robustness* and *security*. Robustness in FL against adversaries that attack a trained model at *test time* by hand-crafted test samples to make the learned model fail the task [8], [11], [31], [45], whereas the security is considered against adversaries that can attack the *training process* with the aim of manipulating the model so that it fails the task at test time. In this work, we focus on the latter.

A brief taxonomy of security threat models. The threat models that target the training/learning process are often described as *poisoning attacks*. We classify them based on three aspects: *activation*, *location*, and *target*. We use the term *activation* to describe attacks that are embedded into the model during training as a *trojan* and activated at test time using a specific triggering signal, which is often referred as a *backdoor attack* [1], [13], [41], [46], [50], or the attack does not require a triggering mechanism, which is often called a *Byzantine attack* [2], [6], [15]–[17], [24], [25], [51], [52]. The second aspect is the *location* of the interaction of the attack with the learning process. When a poisoning attack interacts with the learning process through the training data, we describe it as a *data poisoning attack*, whereas if the attack directly interacts with the model, e.g., through the local model/gradient update in FL, we describe it as a *model poisoning attack*. The last aspect we consider is whether the attack is *targeted*; that is, failure of the learning is desired for a particular type of test data (for instance in classification tasks, certain classes might be the target), or *untargeted*; that is, the failure of the task is desired for any possible test data.

Attacks can also be classified based on their knowledge

of the learning process (white box / black box), or on their capability and control over the system. For further discussion on the taxonomy of poisoning attacks, we refer the reader to [1], [4], [43].

Scope and Contributions. In this work, we focus on untargeted model poisoning attacks, as they are the most effective against FL to disrupt the collaborative learning process [24], [42]. Various Byzantine attack strategies against FL have been introduced in the literature [1], [2], [17], [42], [51], as well as robust aggregation frameworks that replace federated averaging (FedAVG) [33] for defense against them [6], [15], [16], [24], [25], [52]. One common observation regarding untargeted model poisoning attacks, often valid for other attacks as well, is that it is harder to detect the attack as an outlier when the variance of the honest updates is large. Therefore, when the variance is low, that is, the client updates are more correlated and close to the benign update, the strength of the attack is weak, or the attack can be easily detected as an outlier.

As a direct consequence of the observation above, *variance reduction* techniques for stochastic gradient descent (SGD) can provide protection against Byzantine attacks, in addition to their primary task of accelerating the convergence. Indeed, in [15], the authors have shown that by using local momentum it is possible to improve the robustness of the existing defense mechanisms. They also argue that the use of global momentum does not serve the same purpose. In [24], the authors further extend the use of local momentum, and show that its advantage against Byzantine attacks is two-fold: First, it helps reduce the variance, and thus, leaves less space for an attack to be embedded, and second, the aggregated local momentum from the previous iteration can be utilized as a reference point for the *centered clipping* (CC) mechanism to achieve a robust aggregation rule. Indeed, it has been shown that such a combined mechanism of local momentum and CC demonstrates impressive results against many state-of-the-art (SotA) Byzantine attacks, such as *a little is enough* (ALIE) [2] and *inner product multiplication* (IPM) [51] attacks. This design has been further extended to the *decentralized* framework and combined with other variance reduction techniques [21], [25].

In this work, we show that the CC mechanism gives a false sense of security, and its performance against ALIE and IMP might be misleading. To this end, we show that the existing ALIE and IMP attacks can be redesigned to circumvent the CC defense. We first identify the main vulnerabilities of the CC method, and then, by taking into account certain design aspects of ALIE and IPM, we propose a new Byzantine attack that targets the CC defense. We show numerically that our proposed strategy successfully circumvents the CC defense, as well as other well-known defense mechanisms (i.e., Robust FedAVG (RFA) [37] and Trimmed-Mean (TM) [52]). We then propose an improved defense against the proposed attack and show its effectiveness. The contributions of this work can be summarized as follows:

- We analyze the CC framework and identify its key vulnerabilities.

- By revisiting the known time-coupled attacks ALIE and IPM, and taking into account the vulnerabilities we identified, we introduce a new Byzantine attack called relocated orthogonal perturbation (ROP) that utilizes the broadcasted momentum term to circumvent the CC defense.
- By conducting extensive simulations on various datasets, both with independent and identically distributed (IID) and non-IID distributions, and with different neural network architectures, we show that our proposed the ROP attack is effective against the CC defense, as well as other robust aggregators such as RFA and TM.
- We also introduce a new defense mechanism against the proposed Byzantine attack as well as other Byzantine attacks, achieving the same asymptotic complexity as the CC aggregator. We show the robustness of our proposed defense mechanism for both IID and non-IID data distributions.

II. BACKGROUND AND RELATED WORK

Robust aggregators. Defence mechanisms against the presence of Byzantine agents in collaborative learning and distributed computations has been studied in the literature for nearly 40 years [27]. With the increasing deployment of large-scale systems that employ collaborative learning such as FL, the risks and potential consequences of such attacks also growing [22]. Many robust aggregation methods have been studied to counter possible adversarial clients. Most solutions replace FedAVG [33] with more robust aggregation methods built upon various statistical and geometrical assumptions, such as coordinate-wise median (CM) [52], geometric median [7], [14], [37], and consensus reaching methods like majority voting [3]. However, since these aggregators are based on purely statistical assumptions, their robustness fails against the SotA attacks, in which the adversaries can statistically conceal themselves as benign clients. Furthermore, these assumptions may not hold in real FL implementations, in which the data distributions tend to be heterogeneous across clients. As a result of which, benign clients may be labeled as adversaries, and discarded by the aggregator.

TM [52] has been proposed as an improvement over the CM by calculating the mean after discarding the outliers. RFA [37] addressed the issue for heterogeneous data distributions by employing geometric median in their aggregator. Krum/Multi-Krum [6] calculate a geometric distance from each client to every participating client to score them based on their distances, then discard the clients with the lowest scores. One particular downside of the Krum and Multi-Krum method is that due to the scoring function, they are slower aggregators ($O(k^2)$) compared to other aggregators ($O(k)$), where k denotes the number of clients. Bulyan [16] is proposed to prevent Byzantine clients that target very specific locations in the gradients, while being close to the mean in the rest of the gradient values. Bulyan uses the same selection method in Krum, and then applies TM to the selected subset of clients. Nevertheless, these traditional aggregators discard clients on

the outliers one way or another [24]; therefore, their robustness tends to fail in the case of heterogeneous data distributions. Recently, CC [24] is proposed to aggregate all the participating clients, where outlier gradients are scaled and clipped based on the center that is selected by the aggregator using the history of the previous aggregations. This provides better convergence by not fully discarding the outliers and a natural defense mechanism against Byzantines that can act as an outlier.

Incorporating acceleration frameworks. The momentum SGD [35], [38] has been introduced to accelerate the convergence of the SGD framework and to escape saddle points to achieve a better minima [44], [48]. These advantages of the acceleration methods, particularly momentum SGD, promote their use also in the FL framework, with the possibilities of incorporating momentum locally at the clients and globally at the server [47]. However, in the context of Byzantine resilience, only a limited number of works have analyzed the impact of the momentum SGD. In [15], it has been shown that, in terms of Byzantine resilience, utilizing momentum locally at the clients is better than globally at the PS. In [24], the authors have shown that, besides reducing the variance among the updates, the momentum term from the previous iteration can be also used as a reference for the momentum of the next iteration in order to neutralize Byzantine attacks by performing clipping. However, in this work, we argue that malicious clients can also follow a similar strategy to improve their attack strength, and escape from clipping.

Model poisoning attacks and defenses. We can identify three SotA model poisoning attacks that have often been studied in the literature to circumvent the existing robust aggregators [2], [17], [51]. The common ground of these attacks is that Byzantine clients statistically stay close to the benign clients to prevent easy detection and poison the global model by coupling their attacks across multiple communication rounds. However, these attacks do not consider momentum and directly target the gradient values of the clients. In a recent work [42], the authors show that existing Byzantine-robust FL algorithms are significantly more susceptible to model poisoning attacks, and introduced a divide-and-conquer (DnC) framework to prevent such attacks. Some of the existing defenses for backdoor attacks, such as FLAME [36], offer some level of robustness against untargeted model poisoning attacks; however, they are not designed to prevent SotA time-coupled model poisonings attacks such as ALIE or IPM. Recently proposed FLtrust [9] claims to offer more robustness than TM [52] and Krum [6]; however, unlike other aggregators, FLtrust scheme requires part of the dataset to be preserved at the PS, which may not be possible in most FL applications due to privacy concerns. Finally, proposed model poisoning defenses namely DnC and FLtrust, do not employ either local or global momentum and only consider the gradient values of the clients.

TABLE I
NOTATIONS

Notation	Description
\mathcal{K}	Set of clients
\mathcal{K}_b	Subset of benign clients
\mathcal{K}_m	Subset of malicious clients
k	Number of clients
k_b	Number of benign clients
k_m	Number of Byzantines
γ	Fraction of the Byzantines
T	Number of iterations
η	Learning rate
$\theta_{i,t}$	Model parameters of client i at iteration t
$\mathbf{g}_{i,t}$	Gradient vector of client i at iteration t
$\mathbf{m}_{i,t}$	Momentum vector of client i at iteration t
$\tilde{\mathbf{m}}_t$	Aggregate momentum at time t
$\hat{\mathbf{m}}_t$	Benign aggregate momentum at time t
τ	Radius of the CC aggregator

III. PRELIMINARIES

A. Notation

We use **bold** denote vectors, i.e., \mathbf{v} and capital calligraphic letters, e.g., \mathcal{V} , to denote the sets. We use subscript indexing to identify the particular indices "i" or time "t" iteration in a vector or a matrix, i.e., \mathbf{v}_i is the i^{th} element of vector \mathbf{v} or \mathbf{v}_t is the vector \mathbf{v} at iteration t . We generally denote both index and time in subscript i.e., $\mathbf{v}_{i,t}$, particularly when it is changing over time/iterations. We use $\|\cdot\|_k$ norm of a vector; in this paper we use l_2 and l_1 norm, and usage of $\|\cdot\|$ without k corresponds to l_2 norm. We use $\langle \cdot \rangle$ for the inner product between two vectors or matrices. We include Table I to list the variables that are widely used in this paper.

B. Federated Learning (FL)

The objective of FL is to solve the following parameterized optimization problem over k clients in a distributed manner

$$\min_{\theta \in \mathbb{R}^d} f(\theta) = \frac{1}{k} \sum_{i=1}^k \underbrace{\mathbb{E}_{\zeta_i \sim \mathcal{D}_i} f(\theta, \zeta_i)}_{:=f_i(\theta)}, \quad (1)$$

where $\theta \in \mathbb{R}^d$ denotes the model parameters, e.g., weights of a neural network, $\zeta_{i,t}$ is the randomly sampled mini-batch, \mathcal{D}_i denotes the dataset of client i , and f is the problem-specific empirical loss function. At each iteration of FL, each client aims to minimize its local loss function $f_i(\theta)$ using *SGD*. Then, the clients seek a consensus on the model with the help of the PS.

In every communication round t , the PS sends its current model θ_t to every client to synchronize their local models $\theta_{i,t}$. After updating their local models, benign clients first compute gradients $\mathbf{g}_{i,t}$ by randomly sampling a batch $\zeta_{i,t}$, then update their local momentum $\mathbf{m}_{i,t}$, using the local client update scheme, $\mathbf{m}_{i,t} = (1-\beta)\mathbf{g}_{i,t} + \beta\mathbf{m}_{i,t-1}$ to further reduce the variance. The benign client-side of the FL framework corresponds to lines 3-9 of Algorithm 1.

The malicious clients, so-called Byzantines, return a poisoned model to the PS according to a certain predefined attack strategy *Attack*(\cdot) by utilizing all the possible observations

until time t , denoted by \mathcal{H}_t , as illustrated in Algorithm 1 (line 11).

Adversarial model: We assume that the Byzantine clients are omniscient, meaning that they have all the information on the dataset, and can use it to predict the gradients of benign clients, which is in line with other SotA attacks, such as ALIE [2] and IPM [51]. An omniscient Byzantine attacker can also calculate the momentum of the benign clients and store the benign and attacker momentum values to generate an arbitrary momentum and then use it to calculate the benign $\mathbf{m}_{i,t}$ momentum of the respective clients in \mathcal{K}_b . Byzantine attackers are also assumed to know the learning rate η ; and thus can estimate the aggregated momentum value $\tilde{\mathbf{m}}_{t-1}$ generated by the PS. Ultimately, the Byzantine client can utilize this information to create a model poisoning attack in an agnostic manner, i.e., the attacker does not know the aggregator or any deployed defenses used by the PS.

C. SotA model poisonings attacks

In this subsection, we provide a brief overview of the SotA model poisoning attacks that couple their attacks across iterations to increase their impact without being detected.

1) *ALIE*: Traditional aggregators such as Krum [6], TM [52] and Bulyan [16], assume that the selected set of parameters will lie within a ball centered at the real mean within a radius, which is a function of the number of benign clients. In order to circumvent this, the attacker in [2] utilizes index-wise mean ($\bar{\mathbf{m}}$) and standard deviation ($\bar{\sigma}$) vectors of the benign clients to induce small but consistent perturbations to the parameters. By keeping the momentum values close to $\bar{\mathbf{m}}$, ALIE can steadily achieve an accumulation of errors while concealing itself as a benign client during training. To avoid detection and stay close to the center of the ball, ALIE scales $\bar{\sigma}$ with a z^{max} parameter, which is calculated based on the numbers of benign and Byzantine clients. As such, let s be the minimal number $s = \lceil \frac{k}{2} + 1 \rceil - k_m$ of benign clients that are required as “supporters”:

$$z^{max} = z^{max} \left(\phi(z) < \frac{k - k_m - s}{k - k_m} \right) \quad (2)$$

The attacker will then use properties of the normal distribution, specifically the cumulative standard normal function $\phi(z)$, and look for the maximal z^{max} such that the s number of the benign clients will have a greater distance to the mean compared to the Byzantine clients; therefore, those s clients are more likely to be classified as Byzantines.

Ultimately, z^{max} is employed as a scaling parameter for the standard deviation to perturb the mean of the benign clients in set \mathcal{K}_b :

$$\mathbf{m}_i = \bar{\mathbf{m}} - z^{max} \bar{\sigma}, i \in \mathcal{K}_m, \quad (3)$$

where \mathcal{K}_m is the set of Byzantine clients. Each individual Byzantine client generates an attack with a momentum value near $\bar{\mathbf{m}}$, following (3).

2) *IPM*: In [51], the authors approach the problem from a stochastic optimization perspective and highlight the required condition for the convergence of the gradient descent framework that is the inner product between the benign gradient $\bar{\mathbf{g}}$ and the output of the robust estimator should be positively aligned, i.e.,

$$\langle \bar{\mathbf{g}}, AGG(\mathbf{g}_i : i \in \mathcal{K}) \rangle \geq 0, \quad (4)$$

which ensures that the loss is steadily minimized over iterations. Hence, IPM has been designed to break this condition and obstruct convergence. From the attacker’s perspective, the most effective strategy to make (4) invalid is to use the benign gradient values with the inverted signs. However, since most robust aggregators are simply designed to ensure that the output of the robust aggregation will not deviate from the benign gradient, often by using distance to the median as a trust metric, an adversary with $-\bar{\mathbf{g}}$ might be spotted easily. Therefore, the second step of the IPM is to choose the proper scaling parameter to make the adversary stealthy yet effective. Finally, we remark that though at first a glance scaled version of the attack might seem insufficient, the convergence implies $\bar{\mathbf{g}}$ approaches to 0 over iterations; hence, in such a regime accumulation of the adversarial gradients can invalidate condition (4).

D. Robust Aggregators

Several robust aggregation algorithms have been proposed in literature to limit the impact of attacks coupled across the iterations. The CC in [24] algorithm exploits the clipping function f_{CC} to normalize the potential Byzantine client’s momentum that resides far away from a selected reference point. In its form, CC considers $\tilde{\mathbf{m}}_{t-1}$ as the reference point to scale the $\mathbf{m}_{i,t}$ from the clients $i \in \mathcal{K}$. Whether the client is Byzantine or a benign client with very heterogeneous data, f_{CC} scales down and pulls back $\mathbf{m}_{i,t}$ closer to the reference point to ensure a stable update direction, and generates a new stable reference point for the forthcoming iteration:

Algorithm 1 Robust FL with Byzantines

Input: Learning rate η , Aggregator $AGG(\cdot)$, Attack $Attack(\cdot)$

Output: Consensus model: θ_T

```

1: for  $t = 1, \dots, T$  do
2:   Client side:
3:   for  $i = 1, \dots, k$  do in parallel
4:     Receive:  $\theta_{t-1}$  from PS
5:     if  $i \in \mathcal{K}_b$  then
6:       Update local model:  $\theta_{i,t} \leftarrow \theta_{t-1}$ 
7:       Compute SGD:  $\mathbf{g}_{i,t} \leftarrow \nabla_{\theta} f_i(\theta_{i,t}, \zeta_{i,t})$ 
8:       Update Momentum:
9:        $\mathbf{m}_{i,t} = (1 - \beta)\mathbf{g}_{i,t} + \beta\mathbf{m}_{i,t-1}$ 
10:    else
11:       $\mathbf{m}_{i,t} \leftarrow Attack(\mathcal{H}_t)$ 
12:   Server side:
13:   Aggregate local updates:
14:    $\tilde{\mathbf{m}}_t \leftarrow AGG(\mathbf{m}_{1,t}, \dots, \mathbf{m}_{k,t})$ 
15:   Update server model:  $\theta_t \leftarrow \theta_{t-1} - \eta_t \tilde{\mathbf{m}}_t$ 
16:   Broadcast model  $\theta_t$ 

```

Algorithm 2 Aggregation with CC

Inputs: $\tilde{\mathbf{m}}_{t-1}$, $\tilde{\mathbf{m}}_t$, $\{\mathbf{m}_{i,t}\}_{i \in \mathcal{K}}$, $f_{CC}(\cdot)$, τ

- 1: **for** $i = 1, \dots, k$ **do** in parallel
 - 2: $\tilde{\mathbf{m}}_{i,t} = f_{CC}(\mathbf{m}_{i,t} | \tilde{\mathbf{m}}_{t-1}, \tau)$
 - 3: $\tilde{\mathbf{m}}_t = \frac{1}{k} \sum_{i \in \mathcal{K}} \tilde{\mathbf{m}}_{i,t}$
-

$$f_{CC}(\mathbf{m} | \tilde{\mathbf{m}}, \tau) = \tilde{\mathbf{m}} + \underbrace{\min \left\{ 1, \frac{\tau}{\|\tilde{\mathbf{m}} - \mathbf{m}\|} \right\}}_{\delta} (\mathbf{m} - \tilde{\mathbf{m}}).$$

RFA in [37] is a geometric median-based robust aggregation method. The significant difference between RFA and FedAVG is that the former replaces the weighted arithmetic mean with an approximate geometric median; thus limiting the effectiveness of the Byzantine parameters:

$$RFA(\mathbf{m}_1, \dots, \mathbf{m}_k) = \underset{\tilde{\mathbf{m}}}{\operatorname{argmin}} \sum_{i=1}^k \|\tilde{\mathbf{m}} - \mathbf{m}_i\|_2$$

In TM [52]; for each coordinate j , let ω_j denote the sorting of the coordinate values. We compute the average after discarding the k_m largest and smallest values; hence the name trimming. It is considered an improvement over the coordinate-wise median aggregator:

$$[TM(\mathbf{m}_1, \dots, \mathbf{m}_n)]_j = \frac{1}{k-2k_m} \sum_{i=k_{m+1}}^{k-k_{m-1}} [\mathbf{m}_{\omega_j(i)}]_j$$

IV. VULNERABILITIES OF CC

In this section, we identify the limitations of the CC defence mechanism.

A. Relocation of the attack

Existing Byzantine attacks set $\tilde{\mathbf{m}}_t = \frac{1}{k_b} \sum_{i \in \mathcal{K}_b} \mathbf{m}_i$ as a reference to design the attack. Hence, by clipping each individual update according to the previous update direction $\tilde{\mathbf{m}}_{t-1}$, it is possible to reduce the impact of a poisoning attack. Let $\Delta_{i,t}$, $i \in \mathcal{K}_m$, denote the attack vector of Byzantine client i at time t to the mean benign update $\tilde{\mathbf{m}}_t$.

In the CC framework, the benign local momentum and global momentum evolve as follows:

$$\mathbf{m}_{i,t} = \beta \mathbf{m}_{i,t-1} + (1 - \beta) \mathbf{g}_{i,t}, \quad i \in \mathcal{K}_b, \quad (5)$$

$$\tilde{\mathbf{m}}_t = \sum_{i \in \mathcal{K}_b} (\beta \mathbf{m}_{i,t} + (1 - \beta) \mathbf{g}_{i,t}) = \beta \tilde{\mathbf{m}}_{t-1} + (1 - \beta) \sum_{i \in \mathcal{K}_b} \mathbf{g}_{i,t}. \quad (6)$$

Further, let $\tilde{\Delta}_t$ to denote the distance between the reference point at $t-1$, $\tilde{\mathbf{m}}_{t-1}$, and the benign momentum at time t , $\tilde{\mathbf{m}}_t$, i.e.,

$$\tilde{\Delta}_t = \tilde{\mathbf{m}}_t - \tilde{\mathbf{m}}_{t-1}. \quad (7)$$

Existing attacks often target the benign momentum $\tilde{\mathbf{m}}_t$, hence the poisoned updates of the Byzantine client can be written in the following form, with respect to $\tilde{\mathbf{m}}_t$ and $\tilde{\mathbf{m}}_{t-1}$:

$$\begin{aligned} \mathbf{m}_{i,t} &= \tilde{\mathbf{m}}_t + \Delta_{i,t}, \quad i \in \mathcal{K}_m, \\ &= \tilde{\mathbf{m}}_{t-1} + \underbrace{\Delta_t + \Delta_{i,t}}_{\tilde{\Delta}_{i,t}}. \end{aligned} \quad (8)$$

where $\tilde{\Delta}_{i,t}$ is the aggregate form of the attack with respect to the reference point of the CC, $\tilde{\mathbf{m}}_{t-1}$. When $\tilde{\Delta}_{i,t}$ is larger than the radius τ of CC, the aggregation mechanism of CC scales $\tilde{\Delta}_{i,t}$ with $\frac{\tau}{\|\tilde{\Delta}_{i,t}\|}$. Hence, the scaled version of the attack can be written as a sum of two components: one towards $\tilde{\mathbf{m}}_t$ and the second in the direction of the attack i.e.,

$$\tilde{\Delta}_t \frac{\tau}{\|\tilde{\Delta}_{i,t}\|} + \Delta_{i,t} \frac{\tau}{\|\tilde{\Delta}_{i,t}\|}. \quad (9)$$

Hence, when the CC defense is employed, the clipped poisoned update often includes both a benign update and the attack with the corresponding scaling factor in (9). We emphasize that the strength of the attack is directly related to the impact of $\Delta_{i,t}$ in $\tilde{\Delta}_{i,t}$, which eventually determines the effective scaling of the pure attack $\Delta_{i,t}$. Significantly reducing $\tilde{\Delta}_t$ gives the attacker more room to further scale up the perturbation $\Delta_{i,t}$ until $\tilde{\Delta}_t \frac{\tau}{\|\tilde{\Delta}_{i,t}\|} = 1$, while still avoiding clipping. Setting $\Delta_{i,t} \gg \tilde{\Delta}_t$ maximizes the effectiveness of $\Delta_{i,t}$ as it can perturb and poison the PS model by staying close to the center of clipping.

Hence, clipping centered around the previous update direction helps to suppress attacks targeting the current benign update direction. However, the strong aspect of the CC framework also becomes its vulnerability: if the attacker knows the reference point of CC, it only requires the knowledge of the learning rate, which can be easily predicted, to modify the attack accordingly. In other words, the attack can be generated with respect to the reference point, $\tilde{\mathbf{m}}_{t-1}$, and it can easily escape clipping.

We refer to this observation as the *target reference mismatch*, since the target of the attacker, which is often the benign update, is different from the reference of the defense mechanism. We further argue that CC relies on this mismatch and induces a false sense of security. Later, we numerically show how CC can be easily fooled if the attack is revised accordingly. To this end, we consider the *relocation of the attack*, simply targeting the previous update instead of the current benign update. By doing so, we show that the accuracy under the CC defense significantly drops. We will further show that such a strategy is not only successful against CC but also against other SotA defense mechanisms such as TM [52] and RFA [37].

B. Angular Invariance

One of the major drawbacks of CC is the angular invariance against attacks that target the reference point $\tilde{\mathbf{m}}_t$. The CC performs a scaling operation by clipping the client's momentum $\mathbf{m}_{i,t}$ that lies beyond a certain radius. This is achieved by

scaling the gap $\Delta = \mathbf{m}_{i,t} - \tilde{\mathbf{m}}_{t-1}$ with a factor δ , which depends only on its norm $\|\Delta\|$, and it operates as an identity function if $\frac{\tau}{\|\Delta\|} \geq 1$.

Now, consider two vectors $\mathbf{m}_1 = \tilde{\mathbf{m}}_{t-1} + \Delta_1$ and $\mathbf{m}_2 = \tilde{\mathbf{m}}_{t-1} + \Delta_2$, where $\|\Delta_1\| = \|\Delta_2\| \leq \tau$, but $\Delta_1 \neq \Delta_2$. f_{CC} treats \mathbf{m}_1 and \mathbf{m}_2 in an identical manner; however, their angle with respect to reference point $\tilde{\mathbf{m}}$ might be significantly different.

A fundamental question for a fixed norm constraint, $\|\Delta\| \leq \tau$, is how to decide on the attack Δ that has the highest impact? A similar problem is discussed in [51], and from the theoretical analysis of the convergence behaviour, the authors argue that for a given benign momentum $\tilde{\mathbf{m}}$, the aggregated momentum $\tilde{\mathbf{m}}$ is successfully poisoned if

$$\langle \tilde{\mathbf{m}}, \tilde{\mathbf{m}} \rangle < 0, \quad (10)$$

in which case the aggregation framework does not meet the required convergence condition. Accordingly, in [51], the authors propose to use a scaled version of the benign gradient $-\epsilon \tilde{\mathbf{m}}$, $0 < \epsilon < 1$, as a poisoned gradient. However, as highlighted in [24], unless there is a sufficient number of Byzantine clients, it is often difficult to ensure (10). To formally illustrate, considering the naive averaging strategy as aggregator, we have

$$\tilde{\mathbf{m}}_t = \frac{1}{k} \sum_{i \in \mathcal{K}} \mathbf{m}_{i,t} = \frac{1}{k} \left(\sum_{i \in \mathcal{K}_b} \mathbf{m}_i + \underbrace{\sum_{i \in \mathcal{K}_m} \mathbf{m}_i}_{-k_m \delta \tilde{\mathbf{m}}_t} \right), \quad (11)$$

and in the expectation we have

$$\begin{aligned} \mathbb{E}[\tilde{\mathbf{m}}_t] &= \frac{1}{k} (k - k_m(1 + \delta)) \tilde{\mathbf{m}}, \\ &= \left(1 - \frac{k_m}{k}(1 + \delta)\right) \tilde{\mathbf{m}}_t. \end{aligned} \quad (12)$$

Hence, if $\frac{k}{k_m} < (1 + \delta)$, then the expected $\tilde{\mathbf{m}}_t$ will be positively aligned with $\tilde{\mathbf{m}}$. Nevertheless, as shown in [51] (see Theorem 2), when there is certain variation among $\mathbf{m}_{i,t}$, $i \in \mathcal{K}_b$, then IPM can be successful in negatively aligning $\tilde{\mathbf{m}}$ with $\tilde{\mathbf{m}}$. Consequently, under certain conditions on the variation among the true gradients, the IPM attack can be successful. On the other hand, when $k \gg k_m$, on average $\tilde{\mathbf{m}}$ a scaled version of $\tilde{\mathbf{m}}$ with a positive coefficient. To conclude, the impact of the IPM attack is highly dependent on the number of malicious clients and how the benign clients' gradients/updates are aligned with the benign update direction, i.e. benign clients that employ very heterogeneous data. Another drawback of the IPM attack is that, although a scaling parameter is used to hide malicious updates, a defense mechanism that utilizes the angular distance rather than a norm-based distance can easily detect malicious clients.

At this point, we revisit another well-known attack strategy called *ALIE* to highlight the key notions behind our attack strategy. Contrary to IPM, ALIE does not specify a direction for the attack with respect to the benign gradient $\tilde{\mathbf{m}}_t$, but a

constraint on each value of the poisoned gradient with respect to $\tilde{\mathbf{m}}_t$, i.e.,

$$\|\tilde{\mathbf{m}}_t - \mathbf{m}_{i,t}\| \leq \tau, \quad (13)$$

to ensure that the poisoned gradients statistically do not behave as outliers with a proper choice of τ as discussed in Section III-C. Contrary to (12), on average we have

$$\mathbb{E}[\tilde{\mathbf{m}}_t] = \tilde{\mathbf{m}}_t + k_m \Delta \quad (14)$$

Hence, the objective is to perturb the update direction as much as possible without being detected as an outlier. To achieve consistent error accumulation, the attacker must employ similarly aligned perturbation vectors during the training. A common metric for the similarity of two vectors is the *cosine similarity*, which is defined in the following way:

$$\cos(\mathbf{m}_1, \mathbf{m}_2) = \frac{\langle \mathbf{m}_1, \mathbf{m}_2 \rangle}{\|\mathbf{m}_1\|_2 \|\mathbf{m}_2\|_2}. \quad (15)$$

ALIE is quite effective against TM [52], Krum [6], and Bulyan [16] defense mechanisms [2]. Apart from being statistically less visible, ALIE mostly gains from the accumulation of the perturbations over time, which reflects the time-coupled nature of ALIE. We argue that the enabling factor behind the accumulation is the correlation of consecutive attacks; in other words, attack vectors are positively aligned over time, i.e., $\cos(\Delta_t, \Delta_{t-1}) \approx 1$. We emphasize that, even though the attack is formed independently from the benign gradients without specifying a particular direction; however, since it directly utilizes the statistics of the benign clients, which often vary slowly during training, the adversarial perturbations end up being highly correlated over time.

TABLE II
COSINE SIMILARITY FOR THE PERTURBATION VALUES OF THE ALIE ATTACK ON IID CIFAR-10 DATASET. THE AVERAGE COSINE SIMILARITY IS REPORTED OVER 100 EPOCHS (6250 COMMUNICATION ROUNDS).

	$\beta = 0$	$\beta = 0.9$	$\beta = 0.99$
$\cos(\Delta_{t-1}, \Delta_t)$.94	.995	.999

We argue that the direction of the variance $\bar{\sigma}_t$ from benign clients \mathcal{K}_b does not vary significantly during the training period. In Table II, we show that Δ of ALIE is always aligned positively; that is, the perturbation $z^{max} \bar{\sigma}_t$ used by ALIE attack is consistent over iterations in terms its direction. This correlation among attacks over time leads to a stronger accumulation:

Instead, we alternate the sign of Δ_t over consecutive communication rounds, as follows:

$$\Delta_t = \begin{cases} z^{max} \bar{\sigma}_t, & \text{if } t \bmod 2 = 0 \\ -z^{max} \bar{\sigma}_t, & \text{if } t \bmod 2 = 1 \end{cases} \quad (16)$$

ALIE is unable to accumulate error throughout training, leading to normal convergence. We demonstrate the convergence for ALIE and ALIE with alternating sign of Δ in Fig. 1 against the TM aggregator, which is an aggregator that is known not to be robust against ALIE [2]. We indeed observe that ALIE +/−

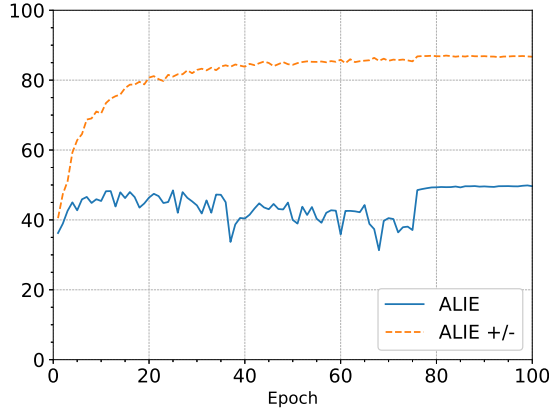


Fig. 1. ALIE attack on TM aggregation, ALIE (blue) denotes the standard ALIE, while ALIE +/- (orange) denotes the version of ALIE where the sign of the perturbation alternates at each communication round.

is not effective against TM, which verifies our argument that its strength comes mainly from the accumulation of attacks over iterations.

Based on the discussion above, for a given norm-bounded attack budget $\|\Delta_t\| \leq r$, we identify two main criteria for the design of an attack:

- Keeping attack positively aligned over time; $\max_{\|\Delta_t\|, \|\Delta_{t-1}\| \leq r} \cos(\Delta_t, \Delta_{t-1})$ to maximize the perturbation accumulated over time.
- Keeping attack orthogonal to the reference update direction $\cos(\Delta_t, \tilde{\mathbf{m}}_t) \approx 0$, which is sufficient to derail the global model, thanks to consistent accumulation over iterations.

Thanks to using small orthogonal perturbations, Byzantine momentum results in $\cos(\tilde{\mathbf{m}}_t + \Delta_t, \tilde{\mathbf{m}}_t) \approx 1$ which is less visible to compared to IPM since Byzantine clients in IPM sends direct opposite of $\tilde{\mathbf{m}}_t$ i.e. $\cos(\mathbf{m}_t, \tilde{\mathbf{m}}_t) \approx -1$.

As we already discussed, the first criterion aims to strengthen the attack by accumulation over time while remaining hard to detected. The second criterion aims to concentrate the accumulated attack orthogonal to the benign update direction in order to derail the model away from the benign optimization path.

Recent works have shown that the use of local momentum helps to decrease the index-wise variation among the parameters of $\mathbf{m}_t \mathbf{m} \in \mathcal{K}_b$, hence improving the robustness against Byzantine clients [15], [24]. We remark that, when the local momentum is employed, achieving the second criterion often implies the first criterion, since the momentum term changes slowly, it remains correlated over time. Hence, an attack strategy is to start with a vector of dimension d and find its orthogonal component to the last update from the server, namely $\tilde{\mathbf{m}}_{t-1}$. Besides being sufficient to derail the model update from its benign trajectory, another advantage of using orthogonal perturbations rather than an attack with stronger perturbation as in IPM, is that it makes it hard to detect malicious clients using cosine similarity-based outlier detection. To illustrate this, we monitor the cosine similarity

TABLE III
AVERAGE COSINE SIMILARITY BETWEEN THE REFERENCE OF CC AND THE BENIGN AND MALICIOUS MOMENTUM, RESPECTIVELY. TRAINED ON THE IID CIFAR-10 DATASET

β	Benign			Byzantine (ROP)		
	0	0.9	0.99	0	0.9	0.99
$\tau=0.1$	0	0.2	0.3	0.94	0.77	0.75
$\tau=1$	-0.03	0.07	0.04	0.48	0.44	0.27

between the reference model, previously aggregated momentum, and the poisoned momentum, and compare it with the average cosine similarity between the reference model and the benign clients' momentum. In Table III, we can observe that the poisoned momentums exhibit a higher cosine similarity with the reference of CC than the average of the benign clients; and hence, any cosine similarity-based defence strategy will further deteriorate the performance rather than successfully detecting malicious updates.

We also remark that using orthogonal perturbations with respect to $\tilde{\mathbf{m}}$ can also be effective against benchmark defense mechanisms and aggregations, especially median-based defenses since those assume benign clients reside close to $\tilde{\mathbf{m}}_t$. However, we consider using orthogonal perturbations with respect to $\tilde{\mathbf{m}}_{t-1}$, because our primary aim is to poison the CC aggregator since in its default CC considers $\tilde{\mathbf{m}}_{t-1}$ as a reference point, thus allowing the attacker to scale up the perturbation even more while avoiding clipping.

V. RELOCATED ORTHOGONAL PERTURBATION (ROP) ATTACK

In order to exploit the aforementioned weaknesses of CC, we introduce a modular and scalable time-coupled model poisoning attack, called *relocated orthogonal perturbation* (ROP). The attack is presented in Algorithm 3. To target the CC aggregator, we relocate the perturbation towards the last update direction $\tilde{\mathbf{m}}_{t-1}$ as a reference point, which corresponds to line 4 in Algorithm 3. Unlike the other robust aggregators that we discussed, CC considers $\tilde{\mathbf{m}}_{t-1}$ as the reference point, as such, Byzantine clients can scale up their perturbation to maximize their effectiveness. After choosing the location of the attack, we consider a direction that is orthogonal to $\tilde{\mathbf{m}}_{t-1}$. To generate an orthogonal perturbation to the reference point, we first take the vector projection of the unit vector $\mathbf{1} \in \mathbb{R}^d$ to the reference point, then subtract the projected vector from the unit vector. After finding an arbitrary orthogonal vector to the reference point, we divide it by its l_2 -norm and scale it with hyper-parameter z to obtain the perturbation vector. These steps correspond to lines [5–8] in Algorithm 3. Although CC does not consider the direction of the attacks, unlike IPM, we avoid using directly opposite direction to the reference point, while still being able to derail the convergence since the opposite direction of attack prevents convergence only if there is a large number of Byzantine clients, otherwise, it only slows down the convergence. Furthermore, Byzantine clients will have similar cosine similarity values to both $\tilde{\mathbf{m}}_{t-1}$ and $\tilde{\mathbf{m}}_t$ compared to the benign clients; preventing

Algorithm 3 ROP Attack

Inputs: $z, \tilde{\mathbf{m}}_{t-1}, \tilde{\mathbf{m}}_t, \Pi$

```

1:  $\mathbf{p} \leftarrow \mathbf{1} \in \mathbb{R}^d$ 
2: if  $t == 1$  then
3:    $\tilde{\mathbf{m}}_{t-1} \leftarrow \tilde{\mathbf{m}}_t$ 
4:  $\mathbf{m}_t \leftarrow \lambda \tilde{\mathbf{m}}_{t-1} + (1 - \lambda) \tilde{\mathbf{m}}_t$ 
5:  $\tilde{\mathbf{p}} \leftarrow \text{Proj}(\mathbf{p}, \mathbf{m}_t)$ 
6:  $\mathbf{p} \leftarrow \mathbf{p} - \tilde{\mathbf{p}}$ 
7:  $\Delta_t \leftarrow \sin(\Pi) \frac{\mathbf{p}}{\|\mathbf{p}\|} + \cos(\Pi) \frac{\mathbf{m}_t}{\|\mathbf{m}_t\|}$ 
8:  $\Delta_t \leftarrow z \Delta_t$ 

```

easy detection by angular defenses that may utilize cosine similarity. By employing a perturbation perpendicular to $\tilde{\mathbf{m}}_{t-1}$ and relocation of the attack towards $\tilde{\mathbf{m}}_{t-1}$, it is effective not only thanks to the accumulation of attacks over iterations, but also because it acts as a catalyst for poisoning history of the CC aggregation. This is because CC considers $\tilde{\mathbf{m}}_{t-1}$ as the center point at time t , thus rop prevents CC from selecting an optimal center point, specifically at *line 2* in Algorithm 2. This is critical since CC itself can further poison its own PS model θ by choosing sub-optimal center locations, which can diminish the effectiveness of actual benign clients by over-clipping or under-clipping the Byzantine clients, and as a result, prevents CC from selecting an optimal reference point to clipping, leading to an increased distance between the optimal $\tilde{\mathbf{m}}_t$ and actual $\tilde{\mathbf{m}}_t$ in the forthcoming communication.

Although the generated perturbation in *line 6* in Algorithm 3 is orthogonal to the selected reference point \mathbf{m}_t , the attacker can change the angle of the attack by the simple operation on \mathbf{m}_t and \mathbf{p} in *line 7* using Π hyper-parameter which can be any angle between $[0-360]$. Byzantine clients can target any "relocated" location for the attack. If Byzantine clients know the deployed defences or the aggregator function used by the PS, attackers can poison the PS more effectively. For example is that if the attacker knows that PS uses a median-based defence mechanism, such as RFA or Median, it can relocate the attack to $\tilde{\mathbf{m}}_t$ to better avoid detection. We finalize the attack structure as:

$$\text{Attack}(\cdot) = \rho \tilde{\mathbf{m}}_{t-1} + (1 - \rho) \tilde{\mathbf{m}}_t + z \Delta_t. \quad (17)$$

We carry out a thorough ablation study in our experiments to understand the effect of the attack location, reference point for perturbation, and angle of the perturbation with respect to the reference point in the supplementary materials.

VI. ROBUSTNESS BY RANDOMIZING THE REFERENCE POINT

In the previous section, we have shown that the predictability of the reference point used for defence mechanisms can lead to certain vulnerabilities. Hence, we argue that the use of a randomized reference point, unlike a static one used in the original CC framework, may enhance the defence framework. Inspired by the recently introduced *bucketing* approach [25], we propose novel variations of the CC framework where the reference momentum changes during the aggregation phase to

Algorithm 4 Sequential centered clipping

Inputs: $\tilde{\mathbf{m}}_{t-1}, \{\mathbf{m}_{i,t}\}_{i \in \mathcal{K}}, f_{CC}(\cdot), \tau$

```

1: Determine number of groups  $R \leftarrow \lceil k/N \rceil$ 
2: Form groups of length  $N$   $\mathcal{C}_1, \dots, \mathcal{C}_R$  by selecting one client from each cluster w.o. repetition.
3: Initialize auxiliary reference momentum:  $\hat{\mathbf{m}}_t = \tilde{\mathbf{m}}_{t-1}$ 
4: for  $n = 1, \dots, \mathbf{do}$ 
5:    $\tilde{\mathbf{m}}_t = \frac{1}{\|\mathcal{C}_n\|} \sum_{i \in \mathcal{C}_n} \tilde{\mathbf{m}}_{i,t}$ 
6:    $\tilde{\mathbf{m}}_t = f_{CC}(\tilde{\mathbf{m}}_{i,t} | \hat{\mathbf{m}}_t, \tau)$ 
7:   if Double Clipping is enabled then
8:      $\tilde{\mathbf{m}}_t = f_{CC}(\tilde{\mathbf{m}}_t | \tilde{\mathbf{m}}_{t-1}, \tau)$ 
9:    $\hat{\mathbf{m}}_t = \tilde{\mathbf{m}}_t$ 
10:  $\tilde{\mathbf{m}}_t = \hat{\mathbf{m}}_t$ 

```

weaken the strength of the Byzantine attack, benefiting the Byzantine clients' collusion. The key objective here is to use a randomized and dynamic reference point instead of a static one as a defence strategy against colluding Byzantines. To this end, we introduce the *sequential CC* (s-CC) framework, presented in Algorithm 4.

A. Sequential Centered Clipping (S-CC)

The key intuition behind the S-CC is to introduce randomness into the CC framework. This is achieved by grouping the clients into buckets of size N , while performing CC in an iterative manner, instead of a single aggregation with a fixed reference point. S-CC performs the aggregation in $\lceil k/N \rceil$ consecutive phases while dynamically updating the reference point at the end of each phase to induce certain randomness to prevent the collusion of the Byzantine clients. Here N is a static hyper-parameter chosen by the PS before the training starts. At the beginning of the aggregation, the clients are sorted by the PS based on cosine similarity between their momentums and the reference point and then divided into N number of clusters. Then, for the aggregation, PS randomly selects one client from each cluster without repetition to form a group and performs CC to update the momentum using the average momentum of the group. Therefore, unlike in the standard CC, the momentum is updated $\lceil k/N \rceil$ times sequentially, while also reducing the total number of clipping operations. It is also possible to employ multiple reference points for the S-CC aggregator, where consecutive f_{cc} operations with different reference points are employed to further clip the momentum of the clients. For double clipping, we consider 2 reference points where first is the dynamic $\hat{\mathbf{m}}_t$ employed in S-CC, and second is the static $\tilde{\mathbf{m}}_t$ employed in the normal CC. In our simulations, we find that double clipping offers near-perfect robustness against ROP; however, it is not stable as S-CC with a single reference point for the ALIE attack.

VII. EXPERIMENTS

A. Datasets and model architectures

We consider two scenarios, where we distribute the data among the clients in IID and non-IID manners, respectively. In the former scenario, we distribute the classes homogeneously among the clients and an equal number of training samples are

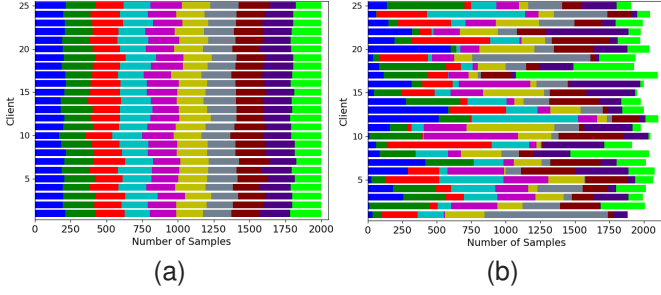


Fig. 2. Visualization of (a) IID and (b) non-IID distribution of 50,000 training samples, 5000 samples per each class, among 25 clients. Each color represents a different class.

allocated to each client. In the non-IID scenario, we partition the whole dataset according to the Dirichlet distribution [34], where the local dataset at each client \mathcal{D}_i has heterogeneous class samples and the total number of samples in each local dataset may vary across the clients. Similar to [43], we use $\text{Dir}(\alpha = 1)$ for the Non-IID scenario, which is more in line with realistic data distributions among distributed clients. Data distributions among 25 clients for the IID and non-IID scenarios are illustrated in Fig. 2.

For the grayscale image classification task, we consider MNIST [28] and FMNIST [49] datasets and train with a 2-layer convolutional neural network (CNN). Due to the relative simplicity of the MNIST dataset, we only consider the non-IID scenario. For the RGB image classification task, we consider CIFAR-10 and CIFAR-100 datasets [26], and train ResNet-20 and ResNet-9 architectures, respectively. However, since CIFAR-100 is a relatively challenging dataset for the image classification task, we only consider the IID scenario for this task.

B. Adversary and FL model

We consider synchronous FL with a total of $k=25$ clients. We assume % 20 of the clients i.e. $k_m=5$ of these are malicious Byzantine clients which is inline with the [24]. For training, we follow a similar setup as in [24], where we train our neural networks for 100 epochs with local batch size of 32 and an initial learning rate of $\eta = 0.1$, which is reduced at epoch 75 by a factor of 0.1. For all the simulations, each local client considers the cross entropy loss to compute gradients.

For simulations with CC, we set its radius to $\tau = [0.1, 1]$ and number of clipping iterations to $l = 1$. We observe that CC is more prone to divergence when $\tau \geq 10$, and since the authors in [24] argue that every τ is equally robust, we only consider these two τ values. For the proposed S-CC aggregator, we consider a cluster size of $N = 3$, and used the average of the clusters for all the simulations.

For the omniscient model poisoning attacks, we consider ALIE, IPM and ROP. In ROP, we experimentally set $z = 1$, $\lambda = 0.9$, $\rho = 1$. The impact of z , λ and ρ on the convergence are further discussed in the supplementary materials. For IPM, we use $\epsilon = 0.2$. For non-omniscient attacks, we consider the bit-flip and label-flip [5], [18] attacks. In the bit-flip attack,

Byzantine clients flip the signs of their own gradient values, whereas in the label-flip attack, Byzantine clients flip the label of a sample by subtracting it from the total number of image classes in the dataset.

C. Numerical Results

In this section, we empirically demonstrate the effectiveness of our proposed ROP attack against robust aggregators, particularly CC with local momentum. For simulations, we compare our proposed ROP with omniscient ALIE [2], IPM [51], and non-omniscient bit-flip and label-flip attacks. In our results, we also report the baseline accuracy of the aggregators, where all the participating clients are benign, i.e. $k_m = 0$. All numerical results are average of 5 runs with different seeds, we report the mean and standard deviation in Table IV.

In Fig 3, we present the effect of ROP and other attacks on the IID FMNIST dataset trained on a 2-layer CNN architecture. Due to the relative simplicity of the dataset and robust CNN architecture, most of the aggregators are capable of fending off the Byzantines in this scenario. Only on $\beta = 0$, ALIE is able to utilize increased variance among the clients, therefore, resulting in the divergence of the RFA and TM aggregators. CC is more robust compared to the other aggregators, however, ROP can still hinder its convergence, especially when local momentum is employed with $\beta = 0.99$, reducing the test accuracy by 5% and 7% for CC with $\tau = 0.1$ and $\tau = 1$, respectively, while also significantly reducing the convergence speed. g the convergence speed.

In Fig 4, we show the convergence behaviour of the ResNet-20 architecture trained on the IID CIFAR-10 dataset. We can observe the effect of time-coupled omniscient attacks like ALIE and ROP. For $\beta = 0$, ALIE can benefit from the increased variance, while ROP can still surpass all the attacks against the CC aggregator. Similar to the results reported in [24], high local momentum benefits all the aggregators; however, ROP is able to achieve low test accuracy by nearly reducing it by 35% in the case of CC with $\beta = 0.99$, which is the best aggregator setup as advised by the authors of CC [24].

For a more challenging setup of aggregators with IID data distribution, we consider the CIFAR-100 image classification task trained on a larger ResNet-9 architecture. The results are given in Fig 5. For CIFAR-100, the RFA aggregator struggles to defend against ROP, ALIE, and IPM on every β parameter, while TM can only converge on $\beta = 0.99$ except of the ROP attack. Against the CC aggregator, without employing a local momentum, time-coupled attacks are capable of derailing the convergence at a certain point, while ROP is capable of hindering the learning process from the start of the training. Similar to the CIFAR-10 results, only ROP can prevent convergence consistently when local momentum is employed, where it can reduce the test accuracy by 40% for $\beta = 0.99$.

In Fig. 6 we show the convergence of aggregators on the MNIST dataset distributed in a non-IID manner. Due to the simplicity of the MNIST dataset, all aggregators can provide normal convergence while employing local momentum. On

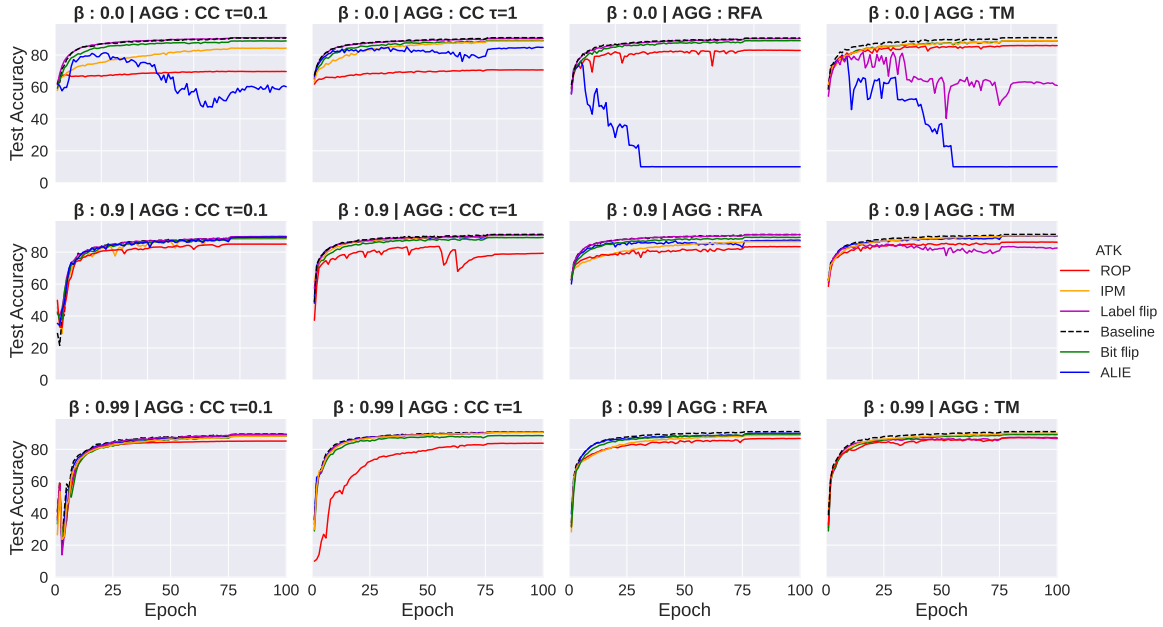


Fig. 3. FMNIST IID test accuracy on various aggregation methods.

$\beta = 0$, ROP can reduce the test accuracy by 20-25 %, while ALIE can diverge the RFA and TM aggregators. In the case of a CC aggregator with $\tau = 0.1$ and $\beta = 0.99$, the PS model cannot achieve the baseline level of the other aggregators even if there is no attacker. We observe that with a large local momentum and non-IID data distribution, CC with low τ fails to converge, which contradicts the claim of the authors in [24] about CC being equally robust for all τ parameters.

In Fig. 7, we show the convergence behavior for the FMNIST dataset distributed in a non-IID manner trained on the same 2-layer CNN architecture. Although FMNIST is a single channel black and white dataset similar to the MNIST, it is considered a more complex dataset which is especially challenging when the dataset’s distribution is very skewed among the clients. In this simulation, ALIE can able to diverge the RFA aggregator while ROP and IPM can able to yield sub-optimal convergence. Interestingly on the TM aggregator, the non-omniscient label-flip attack is the most successful when local momentum is employed. Overall, CC at $\tau = 1$ with local momentum is the most successful aggregator however, ROP can still able to slow down convergence while also lowering the baseline accuracy by almost 20%.

In Fig. 8 we challenge the robust aggregators on the ResNet-20 architecture trained on the CIFAR-10 image classification task with non-IID data distribution. In terms of baseline accuracy i.e., without any attack, CC with $\tau = 0.1$ with local momentum fails to converge, while its IID counterpart and other aggregators can provide normal convergence when there is no Byzantine client. Against all the aggregators and β values, ROP is capable of preventing the convergence from the start of the training meanwhile, with the benefit of the increased variance due to the non-IID data distribution, ALIE

is also a strong competitor to ROP especially when local momentum is not employed however alie assume to know variance thus increased variance greatly helps meanwhile ROP does not assume know the variance yet still surpass the ALIE. In this scenario, TM with $\beta = 0.99$ surpasses the CC aggregator in terms of robustness, although ROP can still reduce the test accuracy by 35%.

Overall, we show that ROP overcomes the robustness of CC regardless of the τ and β parameters, and it is the most successful attack in the IID data distribution scenarios, especially when local momentum is employed. Other attacks fail to prevent the convergence of CC aggregator with $\tau = 1$. In the Non-IID distribution scenario, ALIE is also a successful attack as ROP. This is mainly due to the increased variance among the clients which provides ALIE more room to scale up its perturbation while ROP does not assume to know variance and, uses the same amount of perturbation regardless of the variance among the benign clients. Although in its default configuration, ROP targets the CC, we use the same configuration on a median-based defence TM and a norm-based defence RFA, which both consider statistical calculations using only $\mathbf{m}_{i,t}$ from the clients. We observe that ROP can still compete with and even surpass ALIE. Further analyzing the robust aggregators shows that CC with radius $\tau = 0.1$ is not robust when the data distribution is non-IID and local momentum is employed, failing to converge even when there are no Byzantine clients. This can result from a combination of the low gradient scaling $(1-\beta)$ and very small CC radius τ , which lead to the PS converging very slowly or not learning properly from the clients.

In Fig 9 and 10 we show that the S-CC aggregator can capable of increasing test accuracy for all attack types re-

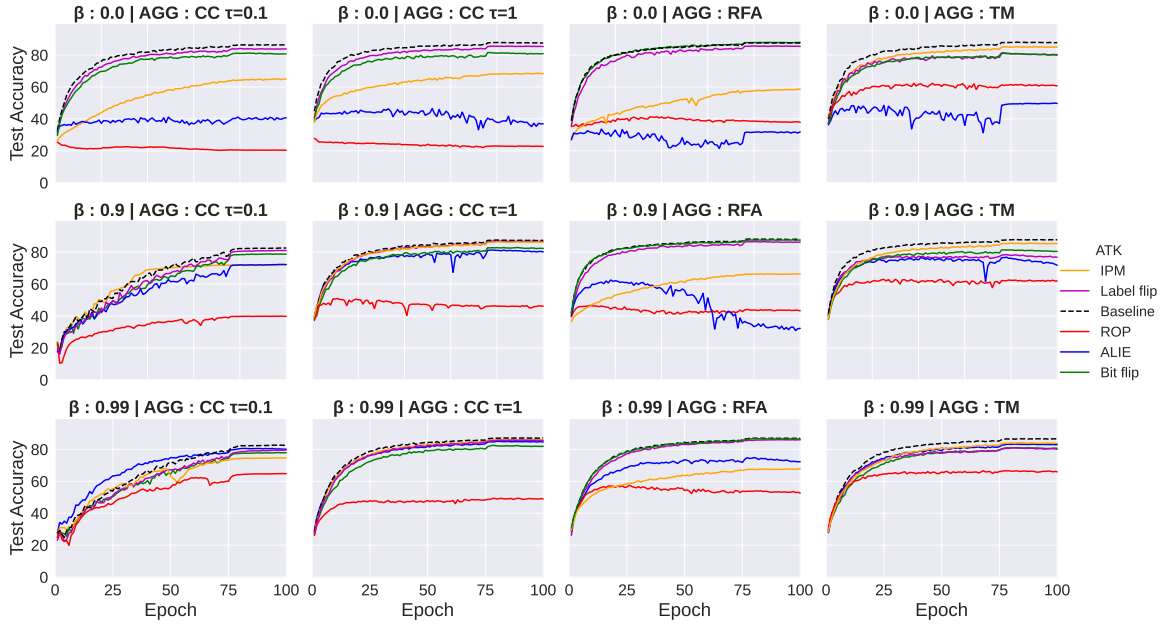


Fig. 4. Cifar10 IID test accuracy on various aggregation methods.

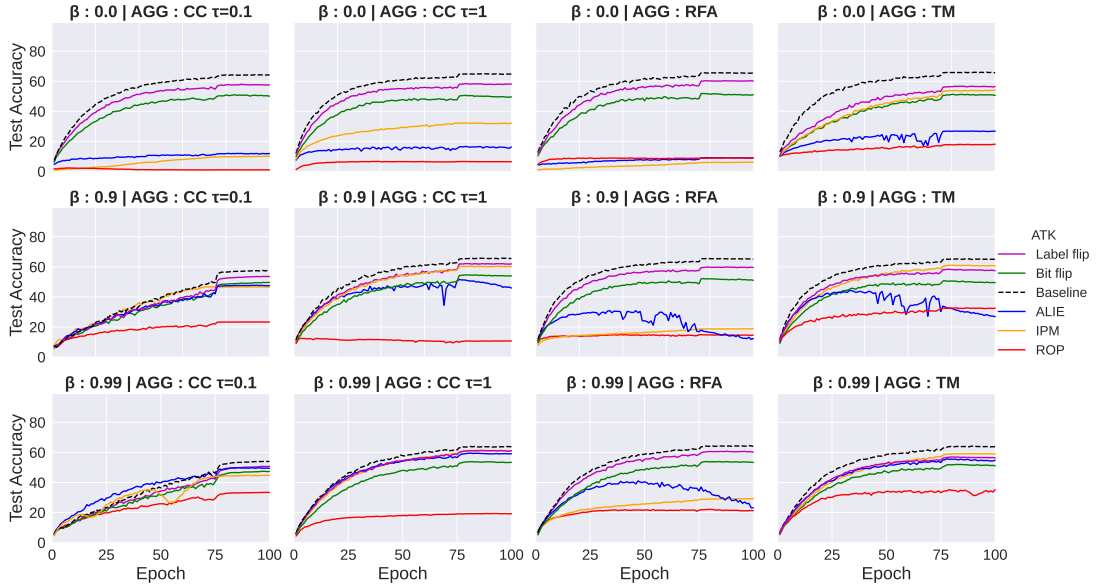


Fig. 5. CIFAR100 IID test accuracy on various aggregation methods.

regardless of the data distribution and β value. Furthermore, for $\beta = 0$ in Fig 9, the S-CC aggregator is equally robust for both IID and non-IID data distribution, which is not the case for every other aggregator that we consider for our simulations. Furthermore, by enabling the double clipping S-CC aggregator can achieve baseline accuracy for ROP attack on any β and data distributions; however, the rest of the attack schemes will result in test accuracy performances that are similar to the CC. However, we consider an aggregator that is robust to all model poisoning attacks while also keeping the same computational complexity of the CC scheme thus we recommend the S-CC

aggregator with local momentum $\beta = 0.9$ where it can achieve near baseline accuracy as seen in Fig. 10.

VIII. DISCUSSION AND CONCLUSIONS

The CC framework in [24] utilizes the acceleration technique of momentum SGD to increase the robustness of the FL framework against Byzantine attacks. The advantage of local momentum is two-fold: First, it decreases the variance of the client updates, statistically reducing the available space for Byzantine attacks. Second, the consensus momentum from the previous iteration can be used to neutralize Byzantine attacks

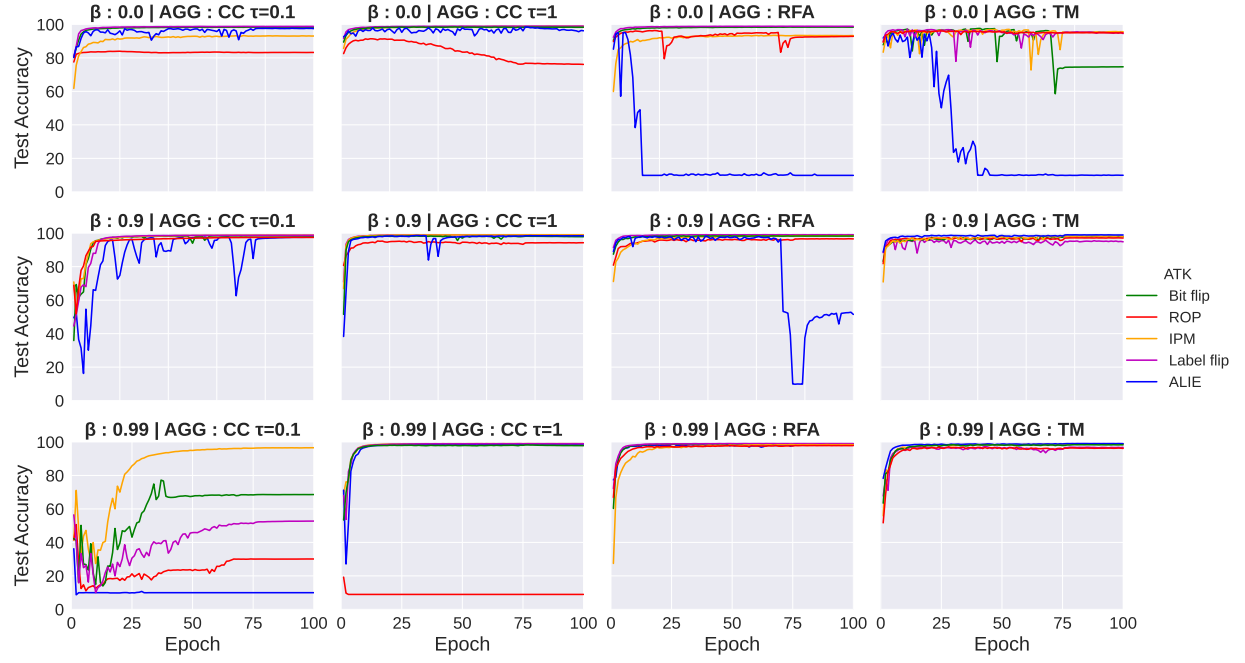


Fig. 6. Mnist Non-IID test accuracy on various aggregation methods.

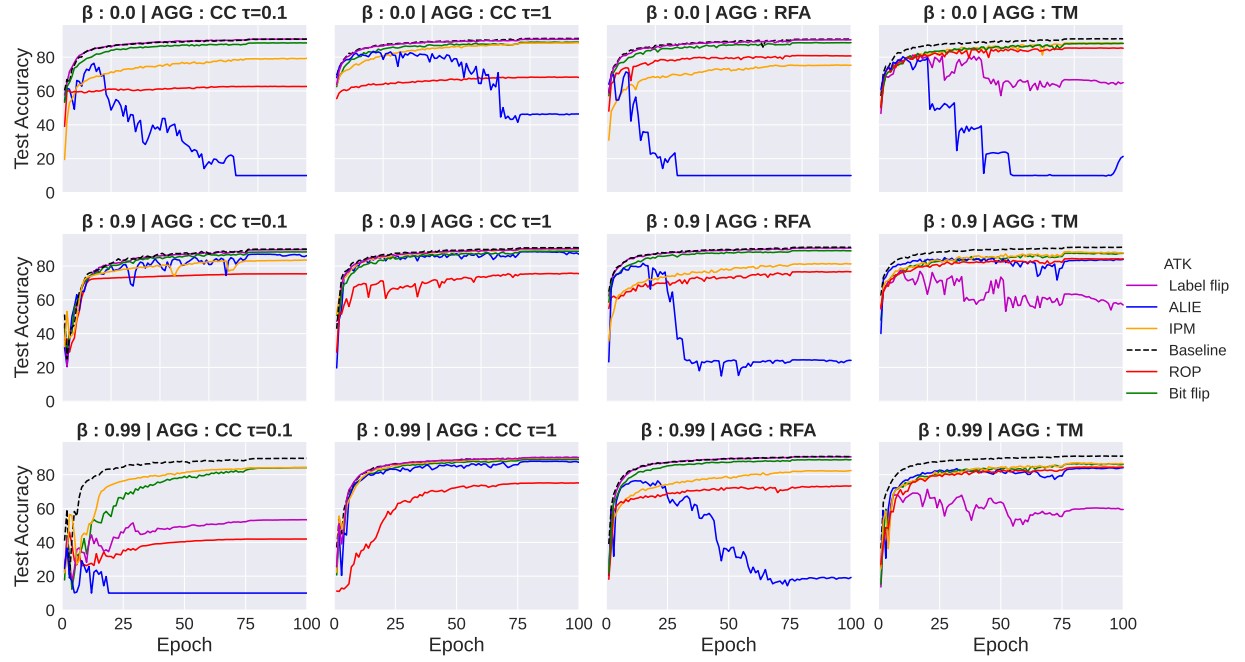


Fig. 7. FMNIST Non-IID test accuracy on various aggregation methods.

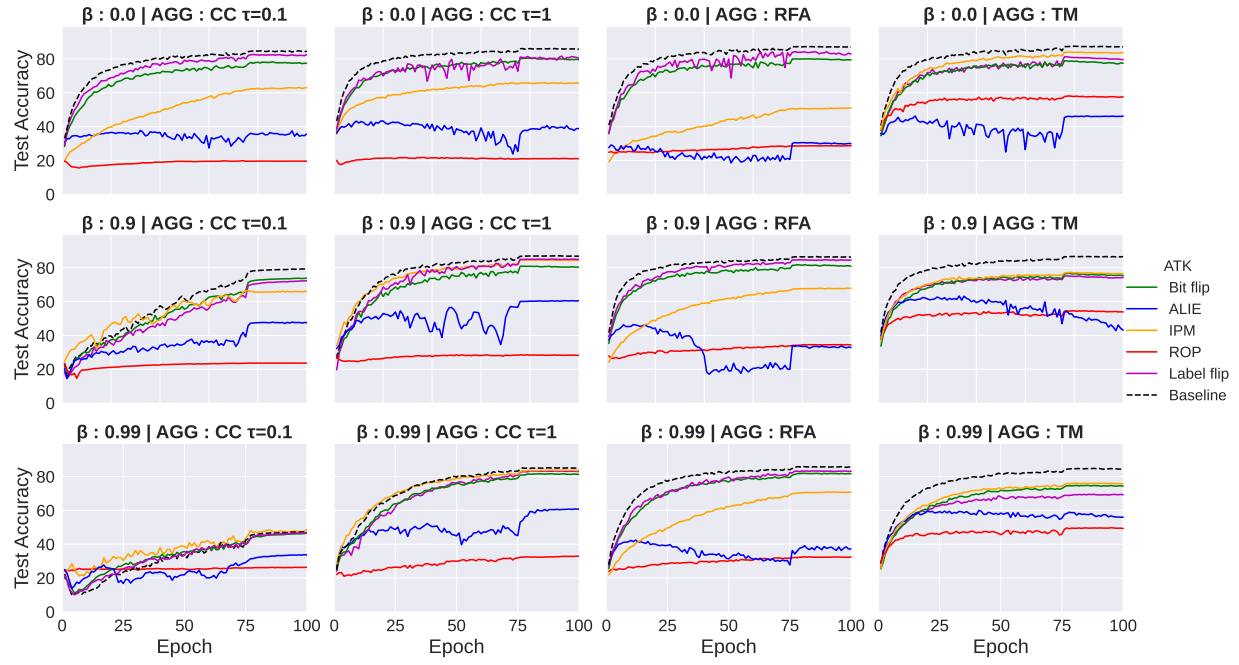


Fig. 8. Cifar10 Non-IID test accuracy on various aggregation methods.

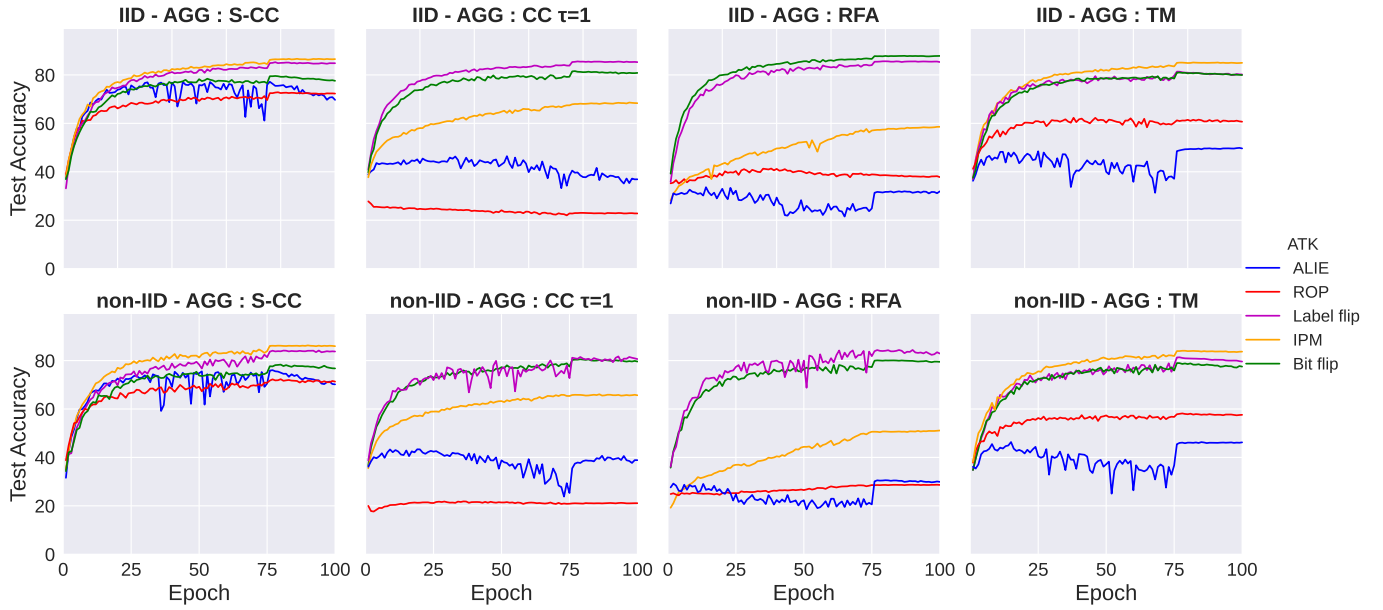


Fig. 9. CIFAR-10 $\beta = 0$ test accuracy on proposed Sequential CC and other aggregators.

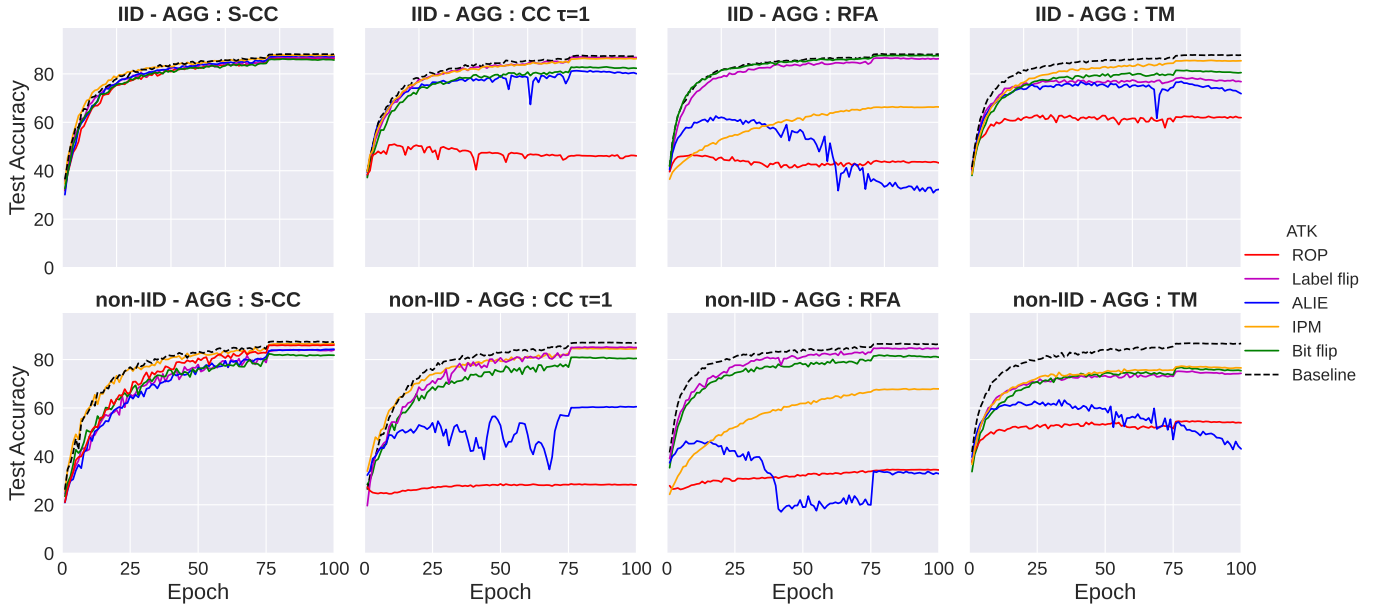


Fig. 10. CIFAR-10 $\beta = 0.9$ test accuracy on proposed Sequential-CC and other aggregators.

by taking it as a reference point and performing clipping accordingly. In this work, we showed that it is possible to circumvent the CC defence by redesigning existing attack mechanisms, such as ALIE and IPM, and that a revised version of these attacks can succeed against other known defence mechanisms.

We highlighted two important aspects of the CC framework. First, Byzantine attacks often target benign updates. However, the CC mechanism considers the previous consensus update as the reference for clipping. Hence, we argue that CC benefits from the mismatch between the target and the reference. Accordingly, it is possible to circumvent CC defences by matching the target and the reference. Second, CC is an angular-invariant operation: the angle between the reference and the candidate does not have an impact on the clipping operation. Based on these observations, we introduced a novel attack mechanism called ROP to circumvent the CC defence. We have shown through extensive numerical experiments that, ROP can successfully poison the model even when CC is used as a defence mechanism. Finally, We have also shown that ROP is also effective against other well-known defence mechanisms, including TM and RFA. We further proposed a potential defence mechanism against ROP, called S-CC. By introducing randomness, through clustering the clients, and dynamically choosing a reference point, the proposed S-CC mechanism offers complete robustness against ROP and drastically improves the test accuracy in the presence of many other known attacks.

REFERENCES

- [1] E. Bagdasaryan, A. Veit, Y. Hua, D. Estrin, and V. Shmatikov, “How to backdoor federated learning,” in *AISTATS*, 2020.
- [2] G. Baruch, M. Baruch, and Y. Goldberg, “A little is enough: Circumventing defenses for distributed learning,” in *NeurIPS*, 2019.
- [3] J. Bernstein, J. Zhao, K. Azizzadenesheli, and A. Anandkumar, “signsgd with majority vote is communication efficient and fault tolerant,” in *ICLR*, 2019.
- [4] A. N. Bhagoji, S. Chakraborty, P. Mittal, and S. Calo, “Analyzing federated learning through an adversarial lens,” in *ICML*, 2019.
- [5] B. Biggio, B. Nelson, and P. Laskov, “Poisoning attacks against support vector machines,” in *ICML*, 2012.
- [6] P. Blanchard, E. M. El Mhamdi, R. Guerraoui, and J. Stainer, “Machine learning with adversaries: Byzantine tolerant gradient descent,” in *NIPS*, 2017.
- [7] —, “Machine learning with adversaries: Byzantine tolerant gradient descent,” in *NIPS*, 2017.
- [8] J. Bruna, C. Szegedy, I. Sutskever, I. Goodfellow, W. Zaremba, R. Fergus, and D. Erhan, “Intriguing properties of neural networks,” in *ICLR*, 2014.
- [9] X. Cao, M. Fang, J. Liu, and N. Z. Gong, “Fltrust: Byzantine-robust federated learning via trust bootstrapping,” in *NDSS*, 2021.
- [10] X. Cao, J. Jia, and N. Z. Gong, “Data poisoning attacks to local differential privacy protocols,” in *USENIX Security*, 2021.
- [11] N. Carlini and D. Wagner, “Towards evaluating the robustness of neural networks,” in *IEEE Symposium on Security and Privacy*, 2017.
- [12] Z. Chai, H. Fayyaz, Z. Fayyaz, A. Anwar, Y. Zhou, N. Baracaldo, H. Ludwig, and Y. Cheng, “Towards taming the resource and data heterogeneity in federated learning,” in *USENIX OpML*, 2019.
- [13] X. Chen, C. Liu, B. Li, K. Lu, and D. Song, “Targeted backdoor attacks on deep learning systems using data poisoning,” *ArXiv*, 2017.
- [14] Y. Chen, L. Su, and J. Xu, “Distributed statistical machine learning in adversarial settings: Byzantine gradient descent,” *Proc. ACM Meas. Anal. Comput. Syst.*, 2017.
- [15] E.-M. El-Mhamdi, R. Guerraoui, and S. Rouault, “Distributed momentum for byzantine-resilient stochastic gradient descent,” in *ICLR*, 2021.
- [16] E. M. El Mhamdi, R. Guerraoui, and S. Rouault, “The hidden vulnerability of distributed learning in byzantium,” in *ICML*, 2018.
- [17] M. Fang, X. Cao, J. Jia, and N. Z. Gong, “Local model poisoning attacks to byzantine-robust federated learning,” in *USENIX Conference on Security Symposium*, 2020.
- [18] C. Fung, C. J. M. Yoon, and I. Beschastnikh, “The limitations of federated learning in sybil settings,” in *23rd International Symposium on Research in Attacks, Intrusions and Defenses (RAID)*, 2020.
- [19] M. Grama, M. Musat, L. Muñoz-González, J. Passerat-Palmbach, D. Rueckert, and A. Alansary, “Robust aggregation for adaptive privacy preserving federated learning in healthcare,” *ArXiv*, 2020.
- [20] A. Hard, K. Rao, R. Mathews, F. Beaufays, S. Augenstein, H. Eichner, C. Kiddon, and D. Ramage, “Federated learning for mobile keyboard prediction,” *ArXiv*, 2018.
- [21] L. He, S. P. Karimireddy, and M. Jaggi, “Byzantine-robust decentralized learning via self-centered clipping,” *ArXiv*, 2022.
- [22] P. Kairouz, H. B. McMahan, B. Avent, A. Bellet, M. Bennis, A. N. Bhagoji, K. Bonawitz, Z. Charles, G. Cormode, R. Cummings *et al.*, “Advances and open problems in federated learning,” *Foundations and Trends® in Machine Learning*, 2021.
- [23] G. A. Kaissis, M. R. Makowski, D. Rückert, and R. F. Braren, “Secure, privacy-preserving and federated machine learning in medical imaging,” *Nature Machine Intelligence*, 2020.
- [24] S. P. Karimireddy, L. He, and M. Jaggi, “Learning from history for byzantine robust optimization,” in *ICML*, 2021.
- [25] —, “Byzantine-robust learning on heterogeneous datasets via bucketing,” in *ICLR*, 2022.
- [26] A. Krizhevsky, V. Nair, and G. Hinton, “Cifar-10 (canadian institute for advanced research).”
- [27] L. Lamport, R. Shostak, and M. Pease, “The byzantine generals problem,” *ACM Trans. Program. Lang. Syst.*, 1982.
- [28] Y. LeCun and C. Cortes, “MNIST handwritten digit database,” 2010. [Online]. Available: <http://yann.lecun.com/exdb/mnist/>
- [29] S. Li, Y. Cheng, Y. Liu, W. Wang, and T. Chen, “Abnormal client behavior detection in federated learning,” *NeurIPS workshop on Federated Learning for User Privacy and Data Confidentiality*, 2019.
- [30] W. Li, F. Milletari, D. Xu, N. Rieke, J. Hancox, W. Zhu, M. Baust, Y. Cheng, S. Ourselin, M. J. Cardoso, and A. Feng, “Privacy-preserving federated brain tumour segmentation,” in *Machine Learning in Medical Imaging*, 2019.
- [31] A. Madry, A. Makelov, L. Schmidt, D. Tsipras, and A. Vladu, “Towards deep learning models resistant to adversarial attacks,” in *ICLR*, 2018.
- [32] M. Malekzadeh, B. Hasircioglu, N. Mital, K. Katarya, M. E. Ozfatura, and D. Gündüz, “Dopamine: Differentially private federated learning on medical data,” *AAAI workshop on Privacy-Preserving Artificial Intelligence (PPAI)*, 2021.
- [33] B. McMahan, E. Moore, D. Ramage, S. Hampson, and B. A. y Arcas, “Communication-efficient learning of deep networks from decentralized data,” in *AISTATS*, 2017.
- [34] T. Minka, “Estimating a dirichlet distribution,” 2000.
- [35] Y. Nesterov, “A method for solving the convex programming problem with convergence rate $o(1/k^2)$,” *Proceedings of the USSR Academy of Sciences*, 1983.
- [36] T. D. Nguyen, P. Rieger, H. Yalame, H. Möllering, H. Fereidooni, S. Marchal, M. Miettinen, A. Mirhoseini, A. Sadeghi, T. Schneider, and S. Zeitouni, “FLGUARD: secure and private federated learning,” *ArXiv*, 2021.
- [37] K. Pillutla, S. M. Kakade, and Z. Harchaoui, “Robust aggregation for federated learning,” *IEEE Transactions on Signal Processing*, 2022.
- [38] B. Polyak, “Some methods of speeding up the convergence of iteration methods,” *USSR Computational Mathematics and Mathematical Physics*, 1964.
- [39] S. Ramaswamy, R. Mathews, K. Rao, and F. Beaufays, “Federated learning for emoji prediction in a mobile keyboard,” *ArXiv*, 2019.
- [40] N. Rieke, J. Hancox, W. Li, F. Milletari, H. Roth, S. Albarqouni, S. Bakas, M. N. Galtier, B. Landman, K. Maier-Hein, S. Ourselin, M. Sheller, R. M. Summers, A. Trask, D. Xu, M. Baust, and M. J. Cardoso, “The future of digital health with federated learning,” *ArXiv*, 2020.
- [41] A. Saha, A. Subramanya, and H. Pirsiavash, “Hidden trigger backdoor attacks,” in *AAAI*, 2020.
- [42] V. Shejwalkar and A. Houmansadr, “Manipulating the byzantine: Optimizing model poisoning attacks and defenses for federated learning,” in *NDSS*, 2021.
- [43] V. Shejwalkar, A. Houmansadr, P. Kairouz, and D. Ramage, “Back to the drawing board: A critical evaluation of poisoning attacks on production federated learning,” in *IEEE Symposium on Security and Privacy*, 2022.
- [44] I. Sutskever, J. Martens, G. Dahl, and G. Hinton, “On the importance of initialization and momentum in deep learning,” in *ICML*, 2013.
- [45] C. Szegedy, V. Vanhoucke, S. Ioffe, J. Shlens, and Z. Wojna, “Rethinking the inception architecture for computer vision,” in *CVPR*, 2016.
- [46] H. Wang, K. Sreenivasan, S. Rajput, H. Vishwakarma, S. Agarwal, J.-y. Sohn, K. Lee, and D. Papailiopoulos, “Attack of the tails: Yes, you really can backdoor federated learning,” *NeurIPS*, 2020.
- [47] J. Wang, V. Tantia, N. Ballas, and M. Rabbat, “SLOWMO: Improving communication-efficient distributed SGD with slow momentum,” in *ICLR*, 2020.
- [48] J.-K. Wang, C.-H. Lin, and J. Abernethy, “Escaping saddle points faster with stochastic momentum,” in *ICLR*, 2020.
- [49] H. Xiao, K. Rasul, and R. Vollgraf, “Fashion-mnist: a novel image dataset for benchmarking machine learning algorithms,” *ArXiv*, 2017.
- [50] C. Xie, K. Huang, P.-Y. Chen, and B. Li, “Dba: Distributed backdoor attacks against federated learning,” in *ICLR*, 2020.
- [51] C. Xie, O. Koyejo, and I. Gupta, “Fall of empires: Breaking byzantine-tolerant sgd by inner product manipulation,” in *Uncertainty in Artificial Intelligence*, 2020.
- [52] D. Yin, Y. Chen, R. Kannan, and P. Bartlett, “Byzantine-robust distributed learning: Towards optimal statistical rates,” in *ICML*, 2018.
- [53] C. Zhang, S. Li, J. Xia, W. Wang, F. Yan, and Y. Liu, “BatchCrypt: Efficient homomorphic encryption for Cross-Silo federated learning,” in *USENIX*, 2020.

APPENDIX

A. Training loss analysis

In this section, we show that the proposed ROP attack prevents aggregators from reaching local minima by converging to saddle points instead. In Fig 11, we show that on IID CIFAR-10, our ROP attack always converges to a saddle point for all aggregators and β values. Unlike ROP, ALIE converges to saddle points at $\beta = 0$ only, which can be explained by increased client variance when worker momentum is not employed. For the non-IID CIFAR10 image classification task, in Fig. 12, we can further see the effects of the high variance for the ALIE attack. Although ALIE can increase its effectiveness when variance is high among the participating clients due to non-IID data distribution, it still has lower training loss on high β values compared to the ROP thus converging to the local minima.

B. Ablation study on ROP attack

In this section, we further illustrate the effects of the hyper-parameters of ROP, namely, λ and z parameters in Algorithm 3.

For the λ hyper-parameter, we grid search the optimal value between $[0, 0.5, 0.9, 1]$ on the IID CIFAR10 image classification problem. In Table V, we show that overall $\lambda = 0.9$ results in the strongest attack for multiple aggregators and β values. We find that $\lambda = 1$ is also quite effective to all aggregator types, meaning that Byzantine clients can generate strong attacks without being omniscient by only employing the broadcasted $\tilde{\mathbf{m}}_{t-1}$ from the PS.

Furthermore, we analyze the location of the attack and the angle of the attack with ρ and π hyper-parameters, respectively. In our extensive simulation results on Table V, we show that relocating the attack to $\tilde{\mathbf{m}}_{t-1}$ has a greater effect on CC while targeting the $\tilde{\mathbf{m}}_t$ can significantly reduce the performance of the RFA. Regarding the angle of the perturbation, $\pi = 90, 120, 135$ are equally capable of diminishing the test accuracy results. By default, ROP employs $\rho = 1$, $\lambda = 0.9$ and $\pi = 90$.

For the z hyper-parameter, we grid search the values $[1, 10, 100]$ and find out that all z values are equally robust to the CC aggregator due to the aforementioned relocation of the attack and angular invariance of the CC in Section IV. On the TM aggregator, we find that an increased z value increases the robustness of the attack considerably compared to the other aggregators. We report our CIFAR-10 image classification task results for IID and non-IID data distributions in Fig. 13 and Fig. 14, respectively.

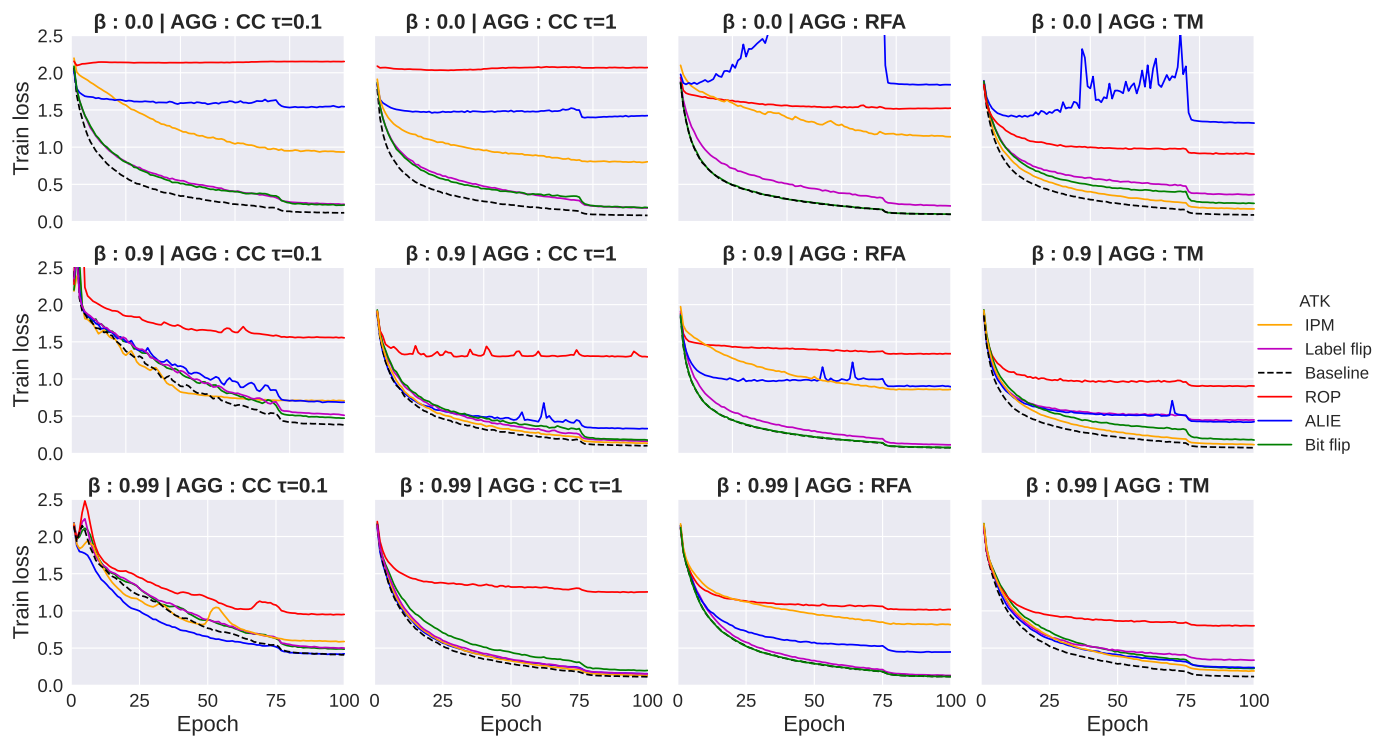


Fig. 11. Cifar10 IID train loss on various aggregation methods.

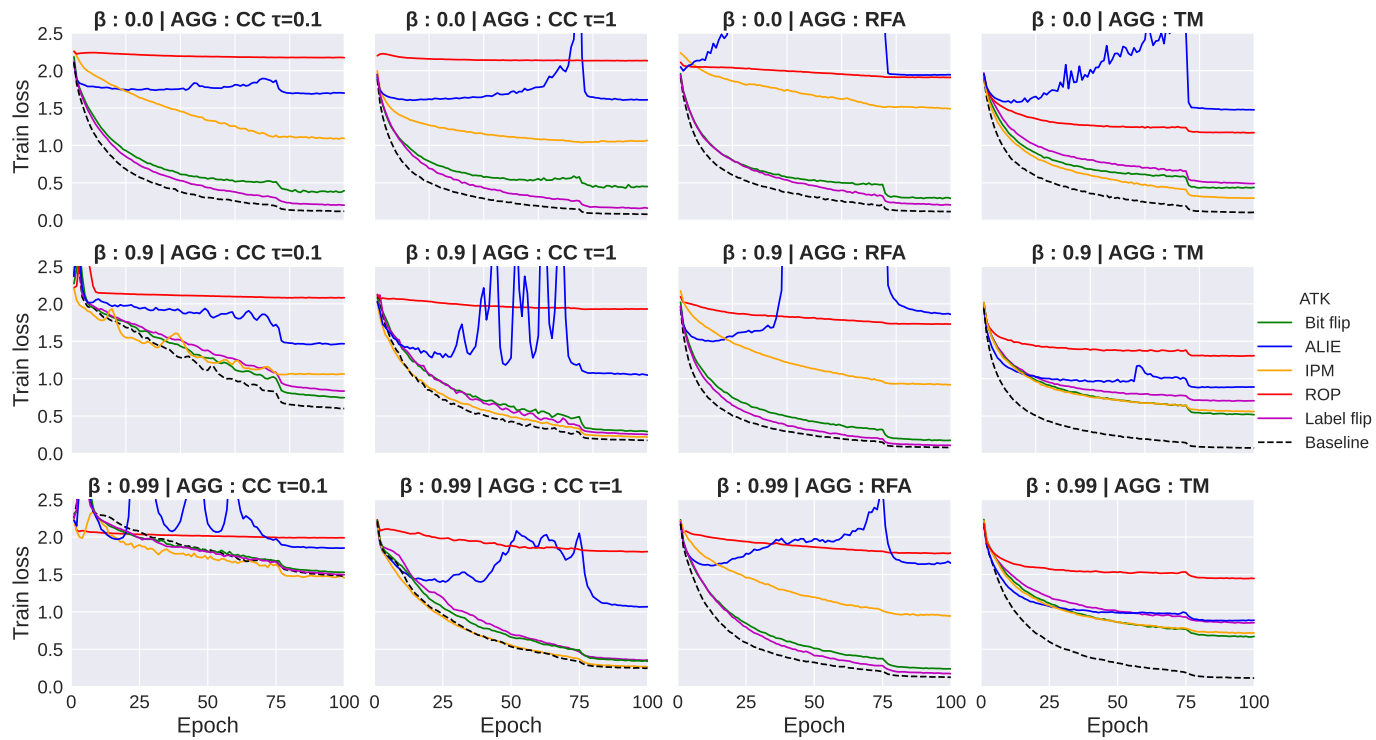


Fig. 12. Cifar10 Non-IID Dir($\alpha=1$) train loss on various aggregation methods.

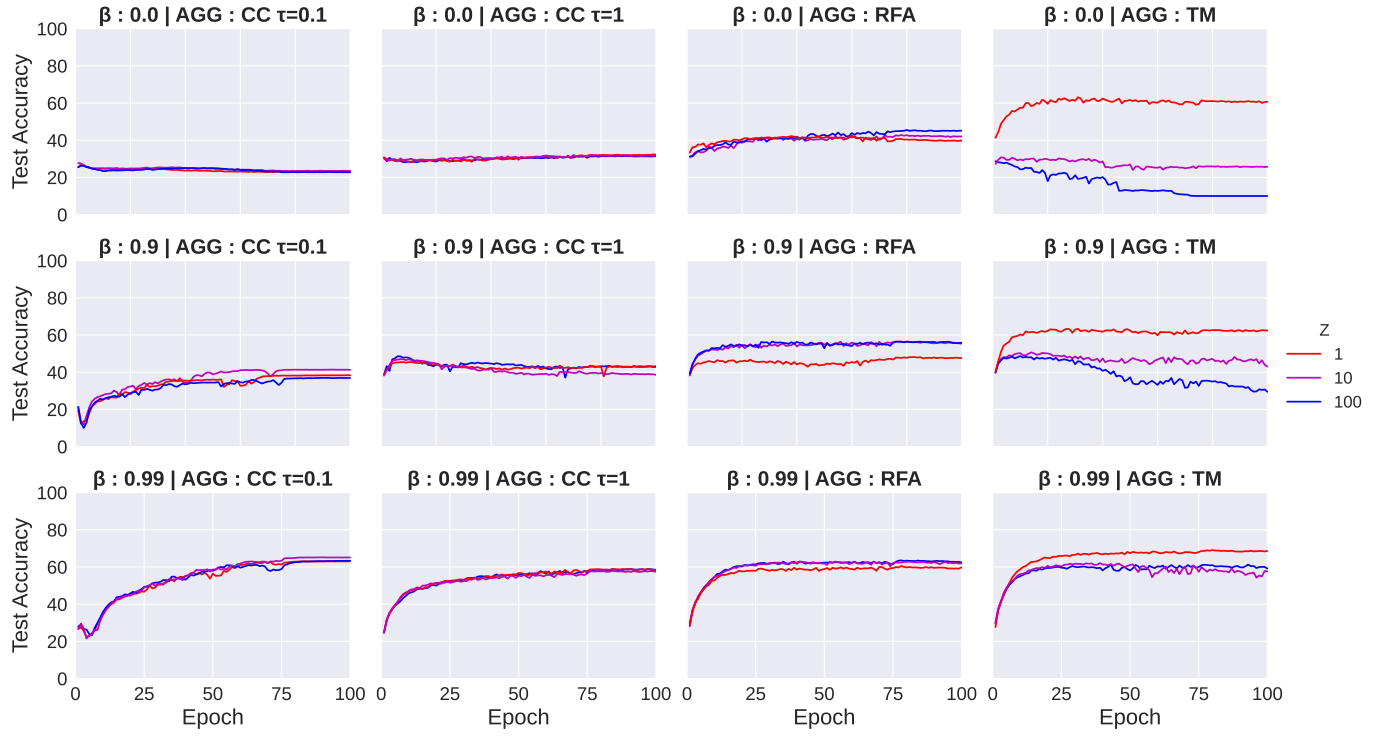


Fig. 13. CIFAR10 test accuracy for ROP attack on various z values for IID distribution.

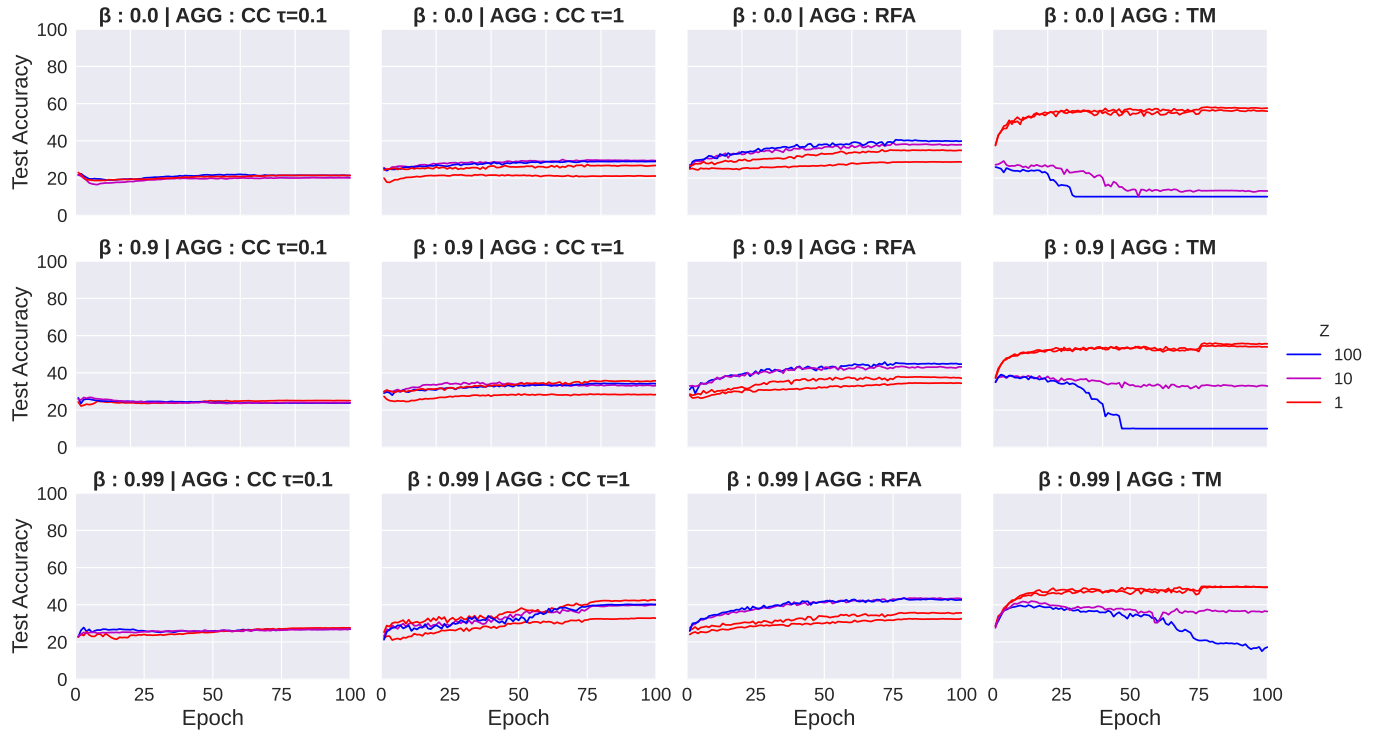


Fig. 14. CIFAR10 test accuracy for ROP attack on various z values for non-IID distribution.

TABLE IV
TEST ACCURACY COMPARISONS ON ALL DATASETS. LOWER IS BETTER. * DENOTES NON-IID DISTRIBUTION.

Dataset	Attack	CC $\tau = 0.1$			CC $\tau = 1$			RFA			TM		
		$\beta=0$	$\beta=0.9$	$\beta=0.99$	$\beta=0$	$\beta=0.9$	$\beta=0.99$	$\beta=0$	$\beta=0.9$	$\beta=0.99$	$\beta=0$	$\beta=0.9$	$\beta=0.99$
FMNIST	ROP	68.52 \pm 0.73	85.02 \pm 1.33	85.17 \pm 1.33	70.63 \pm 0.82	79.31 \pm 7.76	83.8 \pm 1.71	82.85 \pm 0.45	83.45 \pm 0.26	86.81 \pm 0.27	84.43 \pm 2.46	86.2 \pm 0.16	87.24 \pm 0.16
	ALIE	60.14 \pm 17.0	89.42 \pm 0.22	89.16 \pm 0.52	84.8 \pm 0.85	90.55 \pm 0.18	90.71 \pm 0.2	10.0 \pm 0.0	87.43 \pm 1.19	90.1 \pm 0.2	10.0 \pm 0.0	90.08 \pm 0.21	90.72 \pm 0.15
	IPM	84.28 \pm 0.14	88.27 \pm 0.37	88.31 \pm 0.83	88.7 \pm 0.17	90.54 \pm 0.22	90.67 \pm 0.15	80.86 \pm 1.11	86.64 \pm 0.14	88.82 \pm 0.18	88.94 \pm 0.3	90.28 \pm 0.14	90.13 \pm 0.19
	Label flip	90.82 \pm 0.16	89.83 \pm 0.33	89.46 \pm 0.29	90.43 \pm 0.16	90.87 \pm 0.22	90.76 \pm 0.22	90.33 \pm 0.34	90.9 \pm 0.14	90.84 \pm 0.19	60.91 \pm 25.56	82.59 \pm 0.56	86.73 \pm 0.93
	Bit flip	88.79 \pm 0.14	88.88 \pm 0.19	88.34 \pm 0.53	89.11 \pm 0.09	89.19 \pm 0.16	88.5 \pm 0.18	88.97 \pm 0.27	89.28 \pm 0.22	89.56 \pm 0.14	88.82 \pm 0.13	89.3 \pm 0.08	89.22 \pm 0.16
CIFAR10	ROP	20.33 \pm 1.73	39.82 \pm 3	64.75 \pm 0.18	22.79 \pm 1.12	46.15 \pm 1.92	48.91 \pm 0.13	37.8 \pm 0.52	43.25 \pm 2.23	52.6 \pm 1.8	60.7 \pm 0.79	61.93 \pm 0.75	65.9 \pm 0.5
	ALIE	40.68 \pm 2.27	72.24 \pm 0.15	80.1 \pm 0.91	36.89 \pm 9.38	80.09 \pm 1.38	84.59 \pm 0.19	31.9 \pm 1.62	32.26 \pm 16.08	72.26 \pm 1.94	49.64 \pm 1.05	71.83 \pm 2.6	82.9 \pm 0.4
	IPM	64.9 \pm 1.08	72.02 \pm 1.17	74.62 \pm 1.16	68.33 \pm 1.3	86.28 \pm 0.35	85.81 \pm 0.17	58.58 \pm 1.05	66.36 \pm 0.67	67.85 \pm 0.62	85.0 \pm 0.26	85.42 \pm 0.72	83.88 \pm 0.37
	Label flip	83.74 \pm 0.1	81.04 \pm 0.28	79.54 \pm 0.28	85.29 \pm 0.61	86.79 \pm 0.19	85.45 \pm 0.28	85.32 \pm 0.32	86.28 \pm 0.08	85.9 \pm 0.38	80.2 \pm 0.04	76.79 \pm 0.24	80.03 \pm 1.28
	Bit flip	80.62 \pm 0.38	78.72 \pm 0.4	77.87 \pm 0.08	80.84 \pm 0.24	82.32 \pm 1.03	81.88 \pm 0.08	87.85 \pm 0.3	87.5 \pm 0.65	86.31 \pm 0.29	79.95 \pm 0.16	80.53 \pm 0.42	80.69 \pm 0.45
CIFAR100	ROP	1.04 \pm 0.07	23.24 \pm 0.4	33.36 \pm 0.6	6.43 \pm 0.32	10.67 \pm 0.46	19.22 \pm 0.3	9 \pm 0.12	14.56 \pm 0.12	21.18 \pm 0.2	18.1 \pm 0.27	32.5 \pm 1	35.22 \pm 0.76
	ALIE	11.82 \pm 0.04	47.53 \pm 0.38	49.4 \pm 0.86	16.26 \pm 0.1	45.88 \pm 3.68	59.04 \pm 0.48	9.1 \pm 0.35	17.75 \pm 7.07	23.11 \pm 1.41	26.83 \pm 0.32	26.48 \pm 9.63	54.77 \pm 0.4
	IPM	10.06 \pm 2.22	46.56 \pm 2.63	44.78 \pm 0.02	32.0 \pm 0.4	60.22 \pm 0.04	60.95 \pm 0.14	6.1 \pm 3.38	18.76 \pm 0.39	29.2 \pm 0.21	53.97 \pm 0.17	60.6 \pm 0.16	58.88 \pm 0.11
	Label flip	57.52 \pm 0.36	53.58 \pm 0.55	50.72 \pm 0.09	58.16 \pm 0.42	61.95 \pm 0.23	61.08 \pm 0.32	60.12 \pm 0.03	59.55 \pm 0.31	60.2 \pm 0.7	56.48 \pm 0.79	57.4 \pm 0.67	56.38 \pm 0.92
	Bit flip	50.04 \pm 0.44	49.62 \pm 0.22	47.26 \pm 0.4	49.52 \pm 0.91	53.94 \pm 0.11	53.37 \pm 0.45	51.02 \pm 0.55	50.99 \pm 0.02	53.26 \pm 0.24	50.5 \pm 0.68	49.45 \pm 0.73	51.07 \pm 0.02
MNIST *	ROP	82.16 \pm 1.43	97.47 \pm 0.13	9.88 \pm 0.11	78.8 \pm 5.16	95.4 \pm 0.7	97.73 \pm 0.3	91.79 \pm 8.34	96.59 \pm 0.16	97.83 \pm 0.29	95.42 \pm 0.5	97.36 \pm 0.4	97.7 \pm 2.6
	ALIE	97.5 \pm 0.04	97.61 \pm 0.49	9.96 \pm 0.14	96.19 \pm 0.82	98.4 \pm 0.12	98.74 \pm 0.05	9.82 \pm 0.0	51.47 \pm 41.37	98.5 \pm 0.4	9.89 \pm 0.12	98.91 \pm 0.08	99.0 \pm 0.07
	IPM	93.07 \pm 2.78	98.83 \pm 0.04	96.55 \pm 0.59	98.84 \pm 0.09	99.01 \pm 0.03	98.98 \pm 0.01	93.34 \pm 2.74	98.44 \pm 0.11	98.37 \pm 0.28	95.61 \pm 0.9	98.03 \pm 1.23	98.82 \pm 0.07
	Label flip	98.8 \pm 0.0	98.78 \pm 0.02	52.74 \pm 43.0	98.98 \pm 0.0	99.02 \pm 0.03	98.95 \pm 0.02	93.34 \pm 2.74	99.09 \pm 0.15	99.01 \pm 0.08	94.54 \pm 0.57	94.85 \pm 1.14	96.78 \pm 0.46
	Bit flip	98.36 \pm 0.06	98.38 \pm 0.08	68.58 \pm 40.47	98.29 \pm 0.1	97.88 \pm 0.18	97.78 \pm 0.13	98.37 \pm 0.31	98.28 \pm 0.54	98.74 \pm 0.05	74.68 \pm 37.47	97.86 \pm 0.61	98.27 \pm 0.25
FMNIST *	ROP	62.7 \pm 0.9	75.35 \pm 0.88	42 \pm 32	68 \pm 1.35	75.5 \pm 2.61	75.16 \pm 0.4	80.74 \pm 1.6	76.53 \pm 1.35	73.39 \pm 1.8	85.29 \pm 0.37	84.19 \pm 0.37	84.52 \pm 0.34
	ALIE	10.0 \pm 0.0	86.13 \pm 0.41	10.0 \pm 0.0	46.38 \pm 36.38	86.98 \pm 0.34	87.33 \pm 0.96	10.0 \pm 0.0	24.18 \pm 28.35	19.24 \pm 18.47	21.34 \pm 22.69	83.85 \pm 3.57	84.13 \pm 1.52
	IPM	79.34 \pm 0.62	83.43 \pm 1.1	84.18 \pm 0.75	88.44 \pm 0.44	90.17 \pm 0.12	89.97 \pm 0.3	75.28 \pm 2.13	81.23 \pm 1.32	82.46 \pm 1.25	88.33 \pm 0.18	87.61 \pm 1.08	86.55 \pm 1.17
	Label flip	90.77 \pm 0.06	89.7 \pm 0.14	53.38 \pm 35.44	90.55 \pm 0.14	90.23 \pm 0.26	90.13 \pm 0.19	90.27 \pm 0.27	90.61 \pm 0.2	90.59 \pm 0.21	64.97 \pm 28.01	56.9 \pm 23.76	59.43 \pm 24.94
	Bit flip	88.46 \pm 0.27	88.29 \pm 0.48	84.22 \pm 1.33	88.91 \pm 0.28	88.68 \pm 0.21	89.03 \pm 0.41	88.58 \pm 0.21	88.94 \pm 0.16	88.87 \pm 0.2	88.08 \pm 0.49	87.42 \pm 0.26	86.06 \pm 0.87
CIFAR10 *	ROP	21.8 \pm 0.86	23.18 \pm 1.35	18.18 \pm 0.28	19.6 \pm 1	23.64 \pm 1.9	26.36 \pm 1.72	28.64 \pm 1	34.4 \pm 2	32.5 \pm 1.4	57.6 \pm 0.6	53.9 \pm 1.88	49.32 \pm 1.4
	ALIE	35.71 \pm 3.89	47.54 \pm 3.36	33.69 \pm 0.29	38.87 \pm 2.96	60.54 \pm 3.59	60.78 \pm 1.42	29.91 \pm 1.7	32.85 \pm 3.35	37.17 \pm 5.38	46.22 \pm 1.56	43.1 \pm 12.38	56.02 \pm 4.89
	IPM	63.11 \pm 1.1	65.98 \pm 3.11	48.63 \pm 2.79	65.66 \pm 1.26	84.48 \pm 0.73	83.76 \pm 0.44	51.12 \pm 1.72	67.88 \pm 1.91	70.67 \pm 1.23	83.7 \pm 0.77	76.54 \pm 1.7	75.7 \pm 0.37
	Label flip	82.58 \pm 0.58	72.28 \pm 1.52	46.84 \pm 1.16	80.63 \pm 0.02	84.99 \pm 0.45	82.96 \pm 0.81	82.91 \pm 2.86	84.63 \pm 0.03	83.2 \pm 0.57	79.6 \pm 0.73	74.31 \pm 1.12	69.19 \pm 3.06
	Bit flip	77.42 \pm 1.41	73.84 \pm 1.19	46.56 \pm 2.66	79.6 \pm 0.5	80.49 \pm 0.51	81.33 \pm 0.33	79.48 \pm 1.12	80.94 \pm 0.64	81.71 \pm 0.43	77.52 \pm 3.27	75.39 \pm 0.64	74.31 \pm 1.28

TABLE V

HYPER-PARAMETER SEARCH ON ATTACK LOCATION ρ , REFERENCE POINT λ , AND ANGLE OF THE PERTURBATION π W.R.T REFERENCE FOR THE CIFAR-10 IMAGE CLASSIFICATION TASK. THE LOWEST SCORE FOR EACH AGGREGATOR FOR THE RESPECTIVE SIMULATION SETUP IS DENOTED IN **BOLD**

	IID $\beta = 0.9$			IID $\beta = 0.99$			non-IID $\beta = 0.9$		
Atk(.) setup	CC	TM	RFA	CC	TM	RFA	CC	TM	RFA
$\rho = 0, \lambda = 0, \pi = 45$	80.74 \pm 0.0	80.66 \pm 0.18	77.78 \pm 0.78	82.74 \pm 0.02	83.41 \pm 0.11	83.3 \pm 0.11	82.74 \pm 0.02	75.76 \pm 0.9	72.77 \pm 1.38
$\rho = 0, \lambda = 0, \pi = 60$	74.62 \pm 1.76	74.55 \pm 2.34	74.3 \pm 0.55	79.97 \pm 0.39	79.48 \pm 1.18	81.71 \pm 0.38	65.54 \pm 2.6	72.31 \pm 0.46	66.75 \pm 1.51
$\rho = 0, \lambda = 0, \pi = 90$	69.4 \pm 1.76	70.58 \pm 0.34	65.51 \pm 2.02	71.34 \pm 0.37	73.04 \pm 0.36	74.51 \pm 0.27	57.44 \pm 1.4	62.53 \pm 0.28	54.14 \pm 2.06
$\rho = 0, \lambda = 0, \pi = 120$	65.42 \pm 1.84	69.47 \pm 0.92	54.4 \pm 0.88	64.56 \pm 0.05	62.59 \pm 4.93	64.54 \pm 2.28	48.9 \pm 0.54	57.59 \pm 2.26	39.06 \pm 1.27
$\rho = 0, \lambda = 0, \pi = 135$	66.52 \pm 0.06	65.62 \pm 0.5	50.73 \pm 0.12	61.72 \pm 2.34	60.93 \pm 1.77	55.19 \pm 1.42	50.02 \pm 1.18	60.0 \pm 1.85	32.98 \pm 1.61
$\rho = 0, \lambda = 0, \pi = 180$	84.5 \pm 0.28	84.86 \pm 0.18	65.84 \pm 0.14	77.79 \pm 0.06	76.18 \pm 0.74	74.53 \pm 0.16	82.94 \pm 0.06	79.33 \pm 0.7	60.93 \pm 0.75
$\rho = 0, \lambda = 0.5, \pi = 45$	77.24 \pm 0.17	76.5 \pm 0.64	72.42 \pm 0.92	72.68 \pm 0.66	77.36 \pm 1.42	79.49 \pm 0.42	61.24 \pm 1.18	71.7 \pm 1.23	53.06 \pm 3.43
$\rho = 0, \lambda = 0.5, \pi = 60$	73.1 \pm 1.46	69.76 \pm 1.63	66.6 \pm 1.19	68.64 \pm 0.64	74.32 \pm 0.48	74.21 \pm 0.13	56.45 \pm 0.8	64.42 \pm 0.75	41.88 \pm 1.89
$\rho = 0, \lambda = 0.5, \pi = 90$	66.74 \pm 1.14	69.88 \pm 1.32	50.83 \pm 1.74	60.94 \pm 2.08	67.07 \pm 1.66	56.4 \pm 0.97	48.08 \pm 0.18	57.26 \pm 0.43	34.18 \pm 0.7
$\rho = 0, \lambda = 0.5, \pi = 120$	66.86 \pm 0.64	69.27 \pm 0.57	37.09 \pm 0.73	59.77 \pm 1.48	67.43 \pm 1.41	44.65 \pm 1.38	48.96 \pm 0.62	59.13 \pm 1.06	25.15 \pm 2.38
$\rho = 0, \lambda = 0.5, \pi = 135$	66.64 \pm 0.72	70.8 \pm 0.01	30.22 \pm 3.31	60.33 \pm 1.38	63.04 \pm 4.03	50.1 \pm 1.69	47.58 \pm 1.01	59.89 \pm 1.24	22.63 \pm 1.98
$\rho = 0, \lambda = 0.5, \pi = 180$	85.11 \pm 0.25	83.96 \pm 1.0	62.4 \pm 0.86	75.61 \pm 0.81	75.6 \pm 0.4	68.08 \pm 0.94	81.81 \pm 0.71	78.95 \pm 0.94	48.79 \pm 2.98
$\rho = 0, \lambda = 0.9, \pi = 45$	75.0 \pm 1.35	73.44 \pm 0.22	66.34 \pm 1.12	64.78 \pm 0.2	74.76 \pm 0.18	70.66 \pm 1.33	55.48 \pm 2.13	67.68 \pm 1.03	42.87 \pm 1.94
$\rho = 0, \lambda = 0.9, \pi = 60$	69.65 \pm 0.01	70.06 \pm 0.62	53.77 \pm 3.36	56.09 \pm 0.88	70.62 \pm 1.39	60.68 \pm 1.15	45.06 \pm 0.93	63.28 \pm 2.25	42.02 \pm 3.0
$\rho = 0, \lambda = 0.9, \pi = 90$	63.6 \pm 2.12	67.02 \pm 2.43	55.34 \pm 1.72	59.34 \pm 0.48	68.2 \pm 2.56	61.78 \pm 1.86	43.14 \pm 2.15	59.69 \pm 1.42	45.15 \pm 2.04
$\rho = 0, \lambda = 0.9, \pi = 120$	67.51 \pm 0.16	71.4 \pm 1.04	60.86 \pm 0.4	64.02 \pm 1.08	71.14 \pm 1.01	66.65 \pm 0.26	47.54 \pm 1.8	61.98 \pm 2.85	48.15 \pm 0.55
$\rho = 0, \lambda = 0.9, \pi = 135$	69.77 \pm 0.26	74.19 \pm 1.74	64.76 \pm 1.3	70.81 \pm 0.38	71.92 \pm 1.5	71.2 \pm 1.13	54.41 \pm 2.03	65.58 \pm 2.66	55.11 \pm 4.07
$\rho = 0, \lambda = 0.9, \pi = 180$	83.4 \pm 0.15	75.95 \pm 0.22	85.4 \pm 0.2	82.71 \pm 0.28	83.6 \pm 0.72	84.2 \pm 0.28	73.81 \pm 0.76	79.25 \pm 0.25	83.84 \pm 0.46
$\rho = 0, \lambda = 1, \pi = 45$	73.63 \pm 1.3	72.25 \pm 0.24	57.04 \pm 0.46	63.2 \pm 0.96	73.67 \pm 0.52	63.82 \pm 0.95	49.98 \pm 3.24	65.3 \pm 1.51	43.35 \pm 0.44
$\rho = 0, \lambda = 1, \pi = 60$	70.76 \pm 0.64	69.98 \pm 0.62	57.49 \pm 0.5	60.09 \pm 0.32	68.32 \pm 1.47	58.74 \pm 2.35	42.62 \pm 2.6	64.78 \pm 0.43	40.7 \pm 1.8
$\rho = 0, \lambda = 1, \pi = 90$	63.25 \pm 1.15	67.22 \pm 1.9	58.24 \pm 0.02	63.34 \pm 1.15	68.53 \pm 2.8	63.96 \pm 2.37	46.2 \pm 1.1	59.63 \pm 1.78	43.94 \pm 1.02
$\rho = 0, \lambda = 1, \pi = 120$	67.46 \pm 1.54	72.51 \pm 0.31	60.29 \pm 0.72	67.58 \pm 0.63	70.99 \pm 0.33	70.51 \pm 0.93	55.86 \pm 0.3	65.7 \pm 2.44	53.0 \pm 1.89
$\rho = 0, \lambda = 1, \pi = 135$	68.72 \pm 0.8	75.48 \pm 0.53	66.25 \pm 0.62	73.2 \pm 0.78	73.39 \pm 0.21	73.1 \pm 0.43	62.06 \pm 0.72	68.86 \pm 1.31	59.02 \pm 2.18
$\rho = 0, \lambda = 1, \pi = 180$	83.36 \pm 0.62	74.18 \pm 0.57	85.24 \pm 0.04	84.17 \pm 0.36	83.92 \pm 0.09	84.38 \pm 0.16	74.47 \pm 4.82	80.69 \pm 0.77	83.65 \pm 0.35
$\rho = 0.5, \lambda = 0, \pi = 45$	79.2 \pm 1.74	78.75 \pm 0.63	77.94 \pm 0.08	82.5 \pm 0.48	83.84 \pm 0.05	83.66 \pm 0.47	64.54 \pm 0.3	76.36 \pm 1.33	71.34 \pm 1.68
$\rho = 0.5, \lambda = 0, \pi = 60$	73.91 \pm 0.96	73.27 \pm 0.25	73.48 \pm 0.96	78.79 \pm 1.12	79.94 \pm 0.56	81.19 \pm 0.24	62.55 \pm 0.02	67.66 \pm 1.39	65.64 \pm 1.08
$\rho = 0.5, \lambda = 0, \pi = 90$	67.13 \pm 0.24	66.51 \pm 0.7	64.76 \pm 1.29	67.55 \pm 2.8	71.62 \pm 0.8	75.3 \pm 0.35	50.4 \pm 1.56	57.47 \pm 2.15	50.4 \pm 1.71
$\rho = 0.5, \lambda = 0, \pi = 120$	62.43 \pm 0.78	63.54 \pm 1.74	56.21 \pm 0.96	57.65 \pm 0.59	64.9 \pm 1.31	64.27 \pm 1.86	45.53 \pm 2.59	52.5 \pm 3.33	38.24 \pm 2.75
$\rho = 0.5, \lambda = 0, \pi = 135$	64.72 \pm 0.31	63.4 \pm 1.17	55.61 \pm 2.06	56.16 \pm 1.57	58.85 \pm 0.22	59.64 \pm 0.28	42.62 \pm 1.86	55.41 \pm 0.38	34.75 \pm 0.48
$\rho = 0.5, \lambda = 0, \pi = 180$	84.38 \pm 0.14	83.76 \pm 0.3	75.84 \pm 0.12	78.22 \pm 0.42	76.28 \pm 0.47	77.12 \pm 1.06	82.35 \pm 0.36	75.47 \pm 1.1	67.69 \pm 0.08
$\rho = 0.5, \lambda = 0.5, \pi = 45$	75.68 \pm 0.9	73.66 \pm 0.18	67.72 \pm 0.49	68.74 \pm 0.26	77.98 \pm 0.7	79.87 \pm 0.58	57.4 \pm 0.8	66.56 \pm 1.15	55.33 \pm 1.28
$\rho = 0.5, \lambda = 0.5, \pi = 60$	71.44 \pm 0.2	68.34 \pm 1.02	69.12 \pm 0.56	64.46 \pm 0.11	70.82 \pm 2.62	73.99 \pm 1.44	45.32 \pm 0.42	62.47 \pm 1.08	40.93 \pm 0.52
$\rho = 0.5, \lambda = 0.5, \pi = 90$	63.36 \pm 0.9	64.08 \pm 0.35	54.08 \pm 1.4	56.25 \pm 0.32	66.78 \pm 0.45	60.15 \pm 2.1	41.36 \pm 2.2	58.04 \pm 0.76	32.42 \pm 2.11
$\rho = 0.5, \lambda = 0.5, \pi = 120$	59.81 \pm 0.87	67.31 \pm 0.34	40.05 \pm 0.52	52.92 \pm 0.9	65.65 \pm 0.42	48.64 \pm 1.07	39.33 \pm 1.42	58.17 \pm 0.82	27.22 \pm 2.78
$\rho = 0.5, \lambda = 0.5, \pi = 135$	63.23 \pm 0.24	68.01 \pm 0.35	37.77 \pm 3.74	55.47 \pm 1.96	63.97 \pm 0.22	50.86 \pm 3.3	42.0 \pm 0.18	58.03 \pm 1.19	28.53 \pm 1.82
$\rho = 0.5, \lambda = 0.5, \pi = 180$	83.14 \pm 0.0	84.04 \pm 0.9	66.88 \pm 0.36	74.13 \pm 0.22	74.72 \pm 0.66	72.44 \pm 0.42	80.82 \pm 0.4	77.24 \pm 0.61	58.43 \pm 0.58
$\rho = 0.5, \lambda = 0.9, \pi = 45$	70.84 \pm 1.88	71.6 \pm 0.28	68.07 \pm 0.2	62.46 \pm 1.0	73.7 \pm 1.22	72.79 \pm 1.86	41.02 \pm 1.62	63.47 \pm 1.73	38.94 \pm 1.49
$\rho = 0.5, \lambda = 0.9, \pi = 60$	65.84 \pm 0.22	67.81 \pm 0.48	49.15 \pm 5.92	53.92 \pm 0.82	70.62 \pm 0.9	58.2 \pm 3.36	33.94 \pm 0.86	61.6 \pm 0.8	37.58 \pm 2.1
$\rho = 0.5, \lambda = 0.9, \pi = 90$	57.82 \pm 1.56	65.45 \pm 0.66	49.6 \pm 0.68	54.36 \pm 1.68	68.96 \pm 0.04	57.62 \pm 1.72	37.25 \pm 0.76	59.63 \pm 1.3	38.34 \pm 3.65
$\rho = 0.5, \lambda = 0.9, \pi = 120$	57.59 \pm 1.91	69.04 \pm 0.46	54.74 \pm 1.32	63.17 \pm 1.27	68.11 \pm 0.25	62.53 \pm 2.68	38.23 \pm 0.59	59.3 \pm 1.36	40.91 \pm 1.4
$\rho = 0.5, \lambda = 0.9, \pi = 135$	59.22 \pm 0.97	68.9 \pm 0.31	58.1 \pm 1.38	67.46 \pm 0.44	71.56 \pm 1.25	65.13 \pm 2.35	38.83 \pm 2.17	63.68 \pm 1.31	40.49 \pm 1.03
$\rho = 0.5, \lambda = 0.9, \pi = 180$	79.65 \pm 1.06	72.14 \pm 0.77	82.68 \pm 0.14	80.94 \pm 0.8	83.18 \pm 0.54	82.68 \pm 0.0	70.48 \pm 1.19	79.63 \pm 0.94	80.34 \pm 0.45
$\rho = 0.5, \lambda = 1, \pi = 45$	71.42 \pm 0.71	70.6 \pm 0.38	66.76 \pm 1.11	71.42 \pm 0.71	72.82 \pm 0.78	68.27 \pm 2.2	31.82 \pm 1.16	62.89 \pm 1.4	40.73 \pm 1.95
$\rho = 0.5, \lambda = 1, \pi = 60$	64.32 \pm 0.1	66.16 \pm 2.16	51.94 \pm 0.86	56.32 \pm 1.52	67.78 \pm 1.26	59.39 \pm 1.46	36.55 \pm 3.87	57.72 \pm 2.99	39.61 \pm 0.39
$\rho = 0.5, \lambda = 1, \pi = 90$	59.14 \pm 1.2	65.63 \pm 1.44	54.02 \pm 0.74	59.32 \pm 2.04	69.46 \pm 1.3	61.13 \pm 1.53	38.74 \pm 0.5	57.86 \pm 1.37	40.1 \pm 1.72
$\rho = 0.5, \lambda = 1, \pi = 120$	60.86 \pm 0.76	71.09 \pm 0.96	57.49 \pm 0.21	65.48 \pm 2.62	70.2 \pm 0.34	67.14 \pm 1.0	49.18 \pm 0.4	59.7 \pm 1.72	43.98 \pm 2.4
$\rho = 0.5, \lambda = 1, \pi = 135$	65.24 \pm 1.14	73.39 \pm 1.24	59.14 \pm 1.06	70.03 \pm 0.68	70.26 \pm 0.22	68.51 \pm 2.32	56.76 \pm 0.2	62.95 \pm 3.02	44.72 \pm 0.72
$\rho = 0.5, \lambda = 1, \pi = 180$	81.13 \pm 0.08	73.08 \pm 0.08	84.24 \pm 0.14	82.57 \pm 0.5	83.18 \pm 0.72	84.35 \pm 0.08	75.31 \pm 0.48	79.23 \pm 0.97	82.08 \pm 1.04
$\rho = 1, \lambda = 0, \pi = 45$	77.97 \pm 0.59	70.6 \pm 0.38	83.57 \pm 0.39	56.62 \pm 1.14	83.74 \pm 0.34	81.76 \pm 0.3	62.4 \pm 1.27	74.17 \pm 0.65	62.73 \pm 0.4
$\rho = 1, \lambda = 0, \pi = 60$	72.95 \pm 0.81	71.41 \pm 0.16	77.84 \pm 1.2	56.32 \pm 1.52	79.7 \pm 0.1	81.78 \pm 0.35	53.87 \pm 1.48	64.83 \pm 2.02	61.99 \pm 2.75
$\rho = 1, \lambda = 0, \pi = 90$	66.06 \pm 1.54	63.78 \pm 0.45	66.27 \pm 1.93	66.31 \pm 0.06	68.94 \pm 0.22	73.9 \pm 1.06	42.37 \pm 3.8	55.06 \pm 0.52	48.34 \pm 2.59
$\rho = 1, \lambda = 0, \pi = 120$	61.7 \pm 1.29	59.42 \pm 1.96	59.28 \pm 0.42	51.92 \pm 0.0	66.7 \pm 0.14	65.43 \pm 0.37	40.41 \pm 1.84	49.21 \pm 1.06	41.15 \pm 1.27
$\rho = 1, \lambda = 0, \pi = 135$	59.11 \pm 1.46	60.09 \pm 1.01 </							